

Copyright
by
Kwangjun Lee
2015

The Thesis Committee for Kwangjun Lee
Certifies that this is the approved version of the following thesis:

**High intensity resistance training induced angiogenesis
and muscle hypertrophy enhance
skeletal muscle regeneration in volumetric muscle loss rats**

**APPROVED BY
SUPERVISING COMMITTEE:**

Supervisor:

Roger P. Farrar

Matthew R. Brothers

**High intensity resistance training induced angiogenesis
and muscle hypertrophy enhance
skeletal muscle regeneration in volumetric muscle loss rats**

by

Kwangjun Lee, B S.

Thesis

Presented to the Faculty of the Graduate School of
The University of Texas at Austin
in Partial Fulfillment
of the Requirements
for the Degree of

Master of Science in Kinesiology

**The University of Texas at Austin
December 2015**

Dedication

This work is dedicated to my family and friends who have supported and encouraged me.

Abstract

High intensity resistance training induced angiogenesis and muscle hypertrophy enhance skeletal muscle regeneration in volumetric muscle loss rats

Kwangjun Lee, M.S. Kin

The University of Texas at Austin, 2015

Supervisor: Roger P. Farrar

Skeletal muscle has an outstanding regenerative capacity when damaged muscle mass is less than 20%. The volumetric muscle loss (VML) injury, muscle loss beyond self-repair capacity, results in functional and morphological disability. This study investigated the effect of myofibers injection into a decellurized extracellular matrix (ECM) with resistance training on skeletal muscle growth following a VML injury. Male fisher 344 and 2 month old F344-Tg (UBC-EGFP) rats, as myofiber donors, were used in this study. Approximately 20% of the mass of the lateral gastrocnemius (LGAS) was excised, which was replaced by ECM in same dimensions. 30 myofibers were injected into the injury site in 7 days of post injury, Ladder climbing began at 10 days post defect surgery, and rats were subjected to climb a ladder every third day with weight for 6 weeks. Following 56 days of recovery, specific tension of FIB+EXE ($105.77 \pm 3.63 \text{ N/cm}^2$) group was significantly higher than ECM ($82.8 \pm 3.42 \text{ N/cm}^2$) group. EXE ($5122 \pm 92 \mu\text{m}^2$) group increased cross sectional area of intact muscle area significantly compared to ECM ($4668 \pm 79 \mu\text{m}^2$), FIB ($4795 \pm 82 \mu\text{m}^2$), and FIB+EXE ($47642 \pm 97 \mu\text{m}^2$) groups. Quantification of the number of blood vessel larger than

20 μ m in the entire area showed a significant difference only in EXE group (46 ± 4.2) compared to ECM group (35 ± 3.89). EXE group (34 ± 3.2) significantly increased the number of blood vessel compared to ECM group (22 ± 3.3). A significant difference in connective tissue area in middle region of the ECM was quantified between EXE ($45\pm1.6\%$) and ECM ($69\pm1.9\%$) groups. Moreover, small muscle fiber area within ECM was significantly higher in EXE group ($1.39\pm30.15\ \mu\text{m}^2$) than ECM and FIB groups ($0.67\pm0.15\mu\text{m}^2$). The data suggest that ECM transplantation with resistance training can repair a volumetric muscle loss injury by hypertrophy, angiogenesis, and myofiber infiltration through entire ECM regions.

TABLE OF CONTENTS

LIST OF FIGURES.....	x
INTRODUCTION.....	1
LITERATURE REVIEW	
Skeletal Muscle Regeneration Overview	5
The destruction phase	
The repair phase	
The remodeling phase	
Volumetric Muscle Loss overview.....	8
Extracellular matrix as a biological scaffold.....	10
Satellite Cells as a source of muscle reneration.....	12
Myofibers as a Source of Satellite cells.....	14
Resistance Training and Muscle Regeneration.....	15
Innervation and vascularization of the ECM.....	16
SIGNIFICANCE.....	19
METHODS	
Animals.....	20
ECM decellularization.....	20
VML creation & ECM Implantation.....	21
Myofiber Isolation	22
Treatment Surgery.....	22

Exercise Protocol.....	23
Functional Analysis.....	23
Histological Analysis.....	24
Immunohistochemical Analysis.....	25
Imaging and Analysis.....	26
Statistical Analysis.....	26
RESULTS.....	27
DISCUSSION.....	29
APPENDIX A: EXPANDED METHODS	
Extracellular Matrix Decellularization.....	46
Volumetric Muscle Loss Surgery	47
Single Fiber Isolating.....	48
<i>In Situ</i> Functional Analysis.....	49
Hematoxylin & Eosin Staining	51
Masson's Trichrome Staining.....	52
Immunohistochemistry.....	54
APPENDIX B: Raw Data.....	56
REFERENCES.....	62

LIST OF FIGURES

Figure 1: Schematic diagram of surgical procedures in VML injury model.....	32
Figure 2: Surgery and Treatment schedule.....	33
Figure 3: Masson's trichrome staining.....	35
Figure 4: Hematoxylin and eosin staining	36
Figure 5: Cross sectional area in uninjured myofiber.....	37
Figure 6: Neurofilament staining.....	38
Figure 7: Total number of Nerves and size distribution.....	39
Figure 8: PECAM staining.....	40
Figure 9: Number of blood vessel.....	41
Figure 10: Fibrotic tissue density in Middle region of VML.....	42
Figure 11: Small muscle fiber density in Middle region of VML.....	43
Figure 12: Total number of nerve and size distribution in Middle region of VML.....	44
Figure 13: Blood vessel density in Middle region of VML.....	45

Introduction

Skeletal muscles, a bundle of multinucleated and contractile fibers plays a key role in locomotion and structural support (Huard, Li et al. 2002, Juhas and Bursac 2013). Skeletal muscle shows a distinct self-repair capacity in most general injuries. Volumetric muscle loss (VML), however, becomes irreversible because large volume of fibrotic tissues occupies the place originally filled with myofibers. VML resulting in not only loss of muscle mass, but also damage to nerves, blood vessels, and extracellular matrix ECM causes functional deficits, cosmetic flaws, and a permanent handicap (Grogan, Hsu et al. 2011). Surgical free muscle transplantation is a common current treatment of VML, but complete functional and morphological repair remains still a big challenge.

The ECM, a three-dimensional structure that consists of glycoproteins, heparin sulfate proteoglycans, glycosaminoglycans, and type IV collagen, plays a critical role in functional and structural support of skeletal muscles (Clark, McElhinny et al. 2002). The ECM also serves as a storage of growth factors, and the ECM binds to and releases growth factors as well (Schultz and Wysocki 2009). The ECM stores growth factors including fibroblast growth factor (FGF), transforming growth factor- β (TGF- β), hepatocyte growth factor (HGF), and vascular endothelial growth factor (VEGF). Bidirectional interactions between ECM and these growth factors affect wound healing processes. Additionally, released chemokines from degrading ECM following skeletal muscle damage attract progenitor cells and stem cells (Beattie, Gilbert et al. 2008, Mauney, Olsen et al. 2010). Because of those roles of ECM, acellular ECM and biological scaffolds composed with ECM component proteins have been used to repair tissues such as cardiac muscles, skeletal muscle, and abdominal skin (Badyalak, Geddes et al. 2003, Kochupura, Azeloglu et al. 2005).

Especially, acellular ECM scaffolds treated with progenitor cells have been extensively researched in VML injuries (Borschel, Dennis et al. 2004, Kochupura, Azeloglu et al. 2005, Merritt, Cannon et al. 2010). The implantation of a homologous acellular ECM seeded with MSC improved functional recovery after 42 days (Merritt, Cannon et al. 2010). The implantation of acellular ECM with myoblasts repairs abdominal wall defects (Coppi, Bellini et al. 2006), while only homologous acellular ECM implantation results in a large volume of fibrous scar tissues (Conconi, De Coppi et al. 2005).

Satellite cells (SCs), adult stem cells, are primary sources for skeletal muscle regeneration. SCs locating between basal lamina and sarcolemma (Mauro 1961) are mitotically quiescent. Quiescent SCs are characterized by Pax7, paired box7, which plays a key role in SC development and lineage determination. (Allen, Sheehan et al. 1995). Upon exposure to a damage environment, activated SCs start proliferating, they are referred to myoblasts. When SCs enter the differentiation phase, Myogenin and Myf 6 are highly expressed (Grounds, Garrett et al. 1992, Cornelison, Olwin et al. 2000). Myogenin is essential for the fusion of myoblasts either themselves or with existing myofibers. These small myofibers become mature which increase size and express contractile protein such as actin and myosin. Donor cells derived regenerating myofibers are investigated by donor gene expression in host cells Donor SCs not only fuse with themselves or host myofibers, but also exist as SCs within regenerating myofibers through self-renewal (Collins, Olsen et al. 2005, Sacco, Doyonnas et al. 2008). Even though SCs are primary sources contributing skeletal muscle regeneration, enzymatically dissociated and transplanted SCs result in incomplete muscle regeneration due to limited migration, donor-host histocompatibility and early death in a host tissue. Individual, freshly isolated single myofiber transplantation is an alternative

way to deliver SCs to a damaged muscle. SC delivery through individual single fiber transplantation would keep SC stemness because SCs are influenced by the original environment which could increase survival ratio of donor SCs. A single donor myofiber promotes muscle hypertrophy as well as an increase in CSA (Boldrin and Morgan 2013). Transplantation of a single myofiber containing only 7 SCs generates more than 100 new fibers containing 25,000-30,000 myonuclei (Collins, Olsen et al. 2005). Single fiber transplantation also resulted in hypertrophy and high force production. Moreover, donor fiber derived SCs in young age remains in a host muscle permanently which prevents age-related mass reduction (Hall, Banks et al. 2010). A previous study in our lab, transplanting 50 myofibers into pre-embedded ECM results in an increase in the number of regenerating fiber and a decrease in decellularized area in a VML rat.

Resistance training (RT) influences the functional properties in skeletal muscle by modifying fiber structure, mass, metabolism and promoting the release of growth factors. RT potentially induces large muscle mass and high contractile force. Moreover, both resistance and endurance training triggers angiogenesis and vascularization (Green, Goreham et al. 1999, Laughlin and Roseguini 2008).

The vascularization is a particular concern in repairing or regenerating tissues in order to attract residence and circulating cells and provide nutrients and oxygen (Teixeira, Zamuner et al. 2003, Li, Zhu et al. 2007). New myofiber formation should synchronize with vascularization and innervation due to the role of blood vessels and nerves in skeletal muscle. SK-34 muscle derived stem cells triggered regeneration of myofibers, blood vessels, and nerves that were related to functional properties and mass recovery (Tamaki, Uchiyama et al. 2005). Innervation plays an important role in functional morphological skeletal muscle

maintenance. Denervated skeletal muscle continues the path of degeneration due to the failure of neuromuscular junctions which results in atrophy and tissue necrosis (Järvinen, Järvinen et al. 2005). Since denervation results in adverse effects on the muscle, it is essential that regenerating myofibers following VML should accompany with innervation. The role of neurotrophic factors, nerve growth factor (NGF), neurotrophin-3(NT-3), and brain-derived neurotrophic factor (BDNF) in skeletal muscle regeneration has been researched. NGF is an important factor for the survival and growth of neuron. Phenotypic characterization of NGF knockout mice increase in cell death and muscle dystrophy (Ruberti, Capsoni et al. 2000). Muscle-derived stem cells treated with NGF enhances the engraftment efficiency (Yu, Dillon et al. 1999, Lavasani, Lu et al. 2006).

Therefore, the purpose of this study was to determine the effect of regeneration of blood vessel and nerve via single fiber injection with resistance training in a VML rat.

Literature Review

Skeletal Muscle Regeneration Overview

Skeletal muscle consists of a bundle of multinucleated and contractile fibers plays a key role in locomotion and structural support (Huard, Li et al. 2002, Juhas and Bursac 2013). An interaction between neuronal and vascular properties and extracellular matrix is closely related to muscle contractile properties (Huard, Li et al. 2002, Järvinen, Järvinen et al. 2005). The regenerative capacity of skeletal muscle has been widely studied. Even though the recovery time and the level of functional and morphological recovery depend on the type and severity of injury, skeletal muscle has an outstanding regenerative (Huard, Li et al. 2002.) The process of self-regeneration in skeletal muscle can be generally divided into three distinct phases: destruction; repair; and remodeling (Järvinen, Järvinen et al. 2005).

The destruction phase

Skeletal muscle injury causes the rupture of plasma membranes with a calcium influx which activates calcium dependent proteases (Hurme, Kalimo et al. 1991). It leads to disintegration of myofibers and necrosis of the damaged muscle tissues. The damaged skeletal muscle forms a band which prevents the propagation of necrosis toward intact myofibers and repairs the plasma membrane associated damaged area (Järvinen, Järvinen et al. 2005). Neutrophils, the most plentiful type of white blood cells, are recruited initially to the defect area by chemokines including IL-8(CXCL8), MIP-2 (CXCL2) and KC (CSCL1) (Belperio, Keane et al. 2002). The phagocytic neutrophils clear up the debris by proteolytic and oxidative modification (Tidball and Villalta 2010). Activated fibroblasts and macrophages within the injury release chemokines which induce an influx of circulating inflammatory cells. Pro-inflammatory macrophages (M1 macrophages) stimulated by

cytokines such as IFN-gamma, TNF-alpha and LPS (Charge and Rudnicki 2004, Tidball 2005, Juhas and Bursac 2013) follow neutrophils, and migrate to the damaged area through a blood stream to remove debris (Hurme, Kalimo et al. 1991, Cannon and Pierre 1998). Once inflammation has been mitigated, anti-inflammatory macrophages (M2 macrophages) activated by anti-inflammatory cytokines such as interleukine-4, 10 and 13 (Sica and Mantovani 2012) replace M1 macrophages (Arnold, Henry et al. 2007, Chazaud, Brigitte et al. 2009, Rigamonti, Zordan et al. 2014). M2 macrophages attenuate inflammation and tissue degradation by switching the initial injury environment toward a regenerative condition. Inflammatory cells play a role in muscle regeneration as clearing up debris and attracting myogenic precursor cells.

Repair phase

The regeneration of myofibers and the formation of scar tissues are the distinct feature in the repair phase. The repair phase begins with the degeneration phase by the effect of M2 macrophages which activate SCs. Activated SCs proliferate and migrate to the site of injury (Juhas and Bursac 2013). Activated SCs expressing MyoD are characterized by the up-regulation of DNA synthesis and nuclear enlargement (Carlson and Faulkner 1982). Once myoblasts expressing myogenin enter differentiation phase, myoblasts start to fuse with other myoblasts or existing myofibers to form new myofibers (Järvinen, Järvinen et al. 2005, Rigamonti, Zordan et al. 2014). SCs are the primary source contributing new nuclei to the regenerating muscle but SCs are not the only source. The resident muscle-derived stem cells, another population of muscle stem cells, are able to supply myoblasts (Charge and Rudnicki 2004). Furthermore, different types of non-muscle stem cells such as bone marrow stem cells are also capable sources participating in skeletal muscle repair. Bone marrow stem

cells are not only direct sources for myonuclei but also contributors for the muscle SC niche through secretion of paracrine growth factors (Quintero, Wright et al. 2009, Tedesco, Dellavalle et al. 2010)).

Early granulation tissues created by fibroblast is deposited at the site of injury and become a bridge to close the gap between the myofiber stumps providing the strength to resist original tensile forces (Hurme, Kalimo et al. 1991; Järvinen, Järvinen et al. 2005). The infiltrating fibroblasts synthesize ECM component proteins such as collagen and laminin to restore the ECM integrity (Hurme, Kalimo et al. 1991). Unlike most skeletal muscle injuries, volumetric muscle loss forms a dense scar tissue which becomes a barrier hindering the completion of muscle regeneration.

The innervation and vascularization in the regenerating myofibers are crucial steps in the functional recovery of the injured muscles (Grefte, Kuijpers-Jagtman et al. 2007). Angiogenesis, a formation of blood vessels from pre-existing blood vessels, occurs from the adjacent blood vessel branches into the injured tissues by endothelial progenitor cells. Reinnervation of regenerating myofibers is a critical step in order to determine myofiber phenotypes and recover functional capacity (Larkin, Kuzon et al. 2003).

Remodeling phase

The remodeling phase following the repair phase is characterized by myofibers reorganization, scar tissue remodeling and functional recovery. The migration of central located nuclei to the periphery is a maturation process in regenerating myofibers. These maturing myofibers attach to the surrounding ECM and replace the pre-occupied scar tissue. The size of scar tissue decreases as the muscle stumps ingrowth until the regenerating myofibers possibly fuse with the ECM (Kääriäinen, Järvinen et al. 2000, Vaittinen, Hurme

et al. 2002).

These general skeletal muscle repair processes summarized above is not perfectly applied to recovery in large volumetric muscle loss. The VML injured muscle failing a completion of the repair processes results in functional deficits by denervation of the muscle and formation of the large scar tissue (Äärimaa, Kääriäinen et al. 2004, Crow, Haltom et al. 2007). In this study we will examine stem cell administration and resistance training as therapeutic treatments to enhance functional and morphological healing process in VML injuries.

Volumetric muscle loss

Overview

The large volume of skeletal muscle loss usually results in functional deficits, cosmetic flaws, emotional pain and a permanent handicap (Grogan, Hsu et al. 2011). VML arises from not only motor vehicle accidents and surgical ablation such as tumor tissue and diabetic tissue removal in civilians but also, gunshots and explosive substances in military people. This severe loss of full-thickness of a muscle creates a large gap between the end of the transected muscle stumps which hampers the natural regenerative process and triggers fibrosis (Terada 2001). As a result, the pre-occupying connective tissues obstruct myofiber ingrowth and blood vessel infiltration. Since a VML injury results in muscle loss as well as damage to nerves, blood vessels and ECM, completion of functional and morphological repair is still a big challenge. Therefore, the treatments for VML injuries should be concerned about enhancing myogenesis and inhibiting fibrosis at the same time. The proper

scaffolding provides a room for ingrowth new myofibers which are capable to inosculate with remained myofibers. The effect of biological scaffold transplantation with myogenic cells is a prominent research area in regenerative medicine.

Surgical free muscle transplantation is a common current treatment for VML. Not only the treatment often causes donor site morbidity and functional deficits, but also it is not able to apply to the removal of large volumes of muscle tissues (Norris and Kellam 1997, Friedrich, Katolik et al. 2011). Transplanting synthetic scaffolds is an attractive approach because of the high reproducibility and availability. However, synthetic scaffolds also lead some negative effects. Synthetic scaffolds often elicit an excessive inflammatory response and a further complication resulting in failure in incorporation of host tissues (Meintjes, Yan et al. 2011).

Acellular ECM and biological scaffolds composed with ECM components have been used to repair tissues such as cardiac muscles, skeletal muscles, and abdominal skin (Badylak, Geddes et al. 2003, Kochupura, Azeloglu et al. 2005). Acellular ECM preparation involves several processes such as tissues harvest, decellularization, and sterilization. Remaining small amount of DNA in acellular ECM concerns the risk of using xenogenic scaffolds due to immunological rejection. However, researches have shown that ECM component proteins appear highly conserved across species (Gilbert, Freund et al. 2009). In a recent clinical treatment, transplantation acellular porcine ECM to the patient having a skeletal muscle injury in the quadriceps forms new muscle tissues after 36 weeks post recovery, and the patient recovers remarkable contractile properties (Mase Jr, Hsu et al. 2010).

Extracellular matrix as a biological scaffold

The ECM is a three-dimensional structure consisting of glycoproteins, heparin sulfate proteoglycans, glycosaminoglycans, and type IV collagen plays a critical role in functional and structural support of skeletal muscles (Clark, McElhinny et al. 2002). The ECM communicating with cells through integrin subunits regulates activation, proliferation, and differentiation of progenitor cells (Brzóška, Bello et al. 2006). Researches have been shown that the activity in myogenic cells heavily depends on ECM components, especially primary ECM components such as collagen, laminin, and fibronectin have been extensively studied. Agarose hydrogel scaffolds coupled with laminin promotes neurite extension from dorsal root ganglia (Yu, Dillon et al. 1999). The bioengineered hydrogel with collagen and fibrin increase functional properties and cellular hypertrophy (Hinds, Bian et al. 2011). On the other hand, inhibition of collagen synthesis restrains myoblast differentiation (Nandan, Clarke et al. 1990). Myogenic cells cultured on the dish coated with ECM component proteins promote myoblast proliferation and differentiation, especially adhered SCs to laminin increase motility (McFarland, Doumit et al. 1988, Siegel, Atchison et al. 2009, Stern, Myers et al. 2009). Duchenne's muscular dystrophy (DMD), a disease cannot produce dystrophin which makes the sarcolemma brittle, illustrates the importance of ECM protein to muscle structural and function. Patients with DMD result in progressive muscle degeneration that causes premature death.

The elasticity of ECM is one of factors to determine stem cell lineage specification. MSC cultured on collagen coated plates with different elasticity, which mimicked the stiffness of the original tissues, differentiate into neural tissues on a soft plate, myogenic tissues on a medium stiffness plate and bones on a hard plate (Engler, Sen et al. 2006).

While MSC on stiff condition express of smooth muscle cell markers, MSC on soft condition express chondrogenic markers. Moreover, stem cell proliferation also depends on the tissue stiffness. The ratio of MSC' proliferation in respond to TGF- β depended on the matrix stiffness (Park, Chu et al. 2011).

The ECM also serves as a storage of growth factors, and the ECM binds to and releases growth factors as well (Schultz and Wysocki 2009). The ECM stores growth factors including fibroblast growth factor (FGF), transforming growth factor- β (TGF- β), hepatocyte growth factor (HGF), and VEGF. During the repair phase, released chemokines from degrading ECM attract progenitor cells and stem cells (Beattie, Gilbert et al. 2008, Mauney, Olsen et al. 2010). After injures, macrophages and SCs release matrixmetalloproteinases (MMPs) which promote secretion of growth factors binding to ECM, and the growth factors released by ECM enhance progenitor cell migration and proliferation (Hawke and Garry 2001, Lolmede, Campana et al. 2009, Schultz and Wysocki 2009). Cultured SCs under high TGF- β 1 signaling inhibits the MyoD and Myogenin expression resulting in limitation of SC proliferation and differentiation (Li, McFarland et al. 2008). Single myofiber studies show that both HGF and FGF-2 affect SC proliferation (Yablonka-Reuveni, Seger et al. 1999).

Acellular ECM has prominent benefits as a scaffold since antigens, which are able to trigger immune response, are removed, and tissue remodeling macrophages are promoted by acelluar ECM transplantation (Badylak, Valentin et al. 2008). Another benefit of acelluar ECM is biocompatibility and biodegradability which lead host cell to produce their own matrix (Borschel, Dennis et al. 2004). Furthermore, 3D structure of ECM retains the original structure of myofibers, vessels, and nerves which assist myotube alignments and the incorporation with nerves and blood vessels into the ECM (Borschel, Dennis et al. 2004).

Acellular ECM scaffolds seeded with progenitor cells have been extensively researched in VML injuries (Borschel, Dennis et al. 2004, Merritt, Cannon et al. 2010). Blood vessels and myofibers are displayed in an implanted homologous muscle acellular matrix (Marzaro, Conconi et al. 2002). The implantation acellular ECM with myoblasts repairs abdominal wall defects (Coppi, Bellini et al. 2006), while only homologous acellular ECM implantation resulted in a large volume of fibrous scar tissues (Conconi, De Coppi et al. 2005). Previous studies in our lab have shown the ability of the homologous acellular ECM to support muscle and blood vessel regeneration (Merritt, Hammers et al. 2010), while implanting an acellular ECM seeded with mesenchymal stem cells improves functional recovery as well (Merritt, Cannon et al. 2010).

Satellite cells as sources of muscle regeneration

SCs, adult stem cells, are primary sources for skeletal muscle regeneration. SCs locating between basal lamina and sarcolemma are mitotically quiescent. A hall mark of SC is a self-renewing capacity which has been demonstrated by SCs transplantation studies. Transplanted SCs into SC depleted mdx mice not only form myofibers, but also migrate to the host SC niche and incorporated with host fibers (Sacco, Doyonnas et al. 2008). The number of SCs in a single fiber associates with age and fiber types, and SCs are unevenly distributed along a fiber. 30~35% of nuclei in a postnatal mouse express SC markers while an adult mouse consists only 1~4% of SC (Schultz 1974). Soleus, a slow type of muscle has two- to threefold SCs than extensor digitorum longus , a fast type of muscle (Gibson and Schultz 1982, Snow 1983). The population of SC is heterogenous in mammals such as mouse, rat and human (Biressi and Rando 2010, Lindström, Pedrosa-Domellöf et al. 2010,

Rossi, Pozzobon et al. 2010). High density of SC has been observed adjacent to capillaries (Schmalbruch and Hellhammer 1977) and close to motor neuron junction (TENNYSON, KREMZNER et al. 1973) which imply they contribute to SC character. SCs are characterized by distinct markers in each sequential step. Quiescent SCs are characterized by Pax7, paired box7, which plays a key role in SC development and lineage determination. Pax7- null mice appear 50% decrease in body weight at 7 days of age, even pax7-null mice die within 2 weeks after birth (Jostes, Walther et al. 1990, Seale, Sabourin et al. 2000).

Growth factors play a major role in SC proliferation and differentiation. IGF-1 is a well-known growth factor for skeletal muscle regeneration. IGF-1 is able to change the expression of myogenic regulatory factors and elevate the proliferation of SC (Allen and Boxhorn 1989, Charge and Rudnicki 2004). HGF leads SC migration to the site of damage (Bischoff 1997) and SC proliferation by binding to c-met (Allen, Sheehan et al. 1995). In a process of muscle regeneration, SCs exposed to the muscle injury start proliferating by multiple cellular and molecular responses governing SC environment. Activated SCs, they are often referred to myoblasts, are characterized by the upregulation of Myf5 and MyoD (Cornelison and Wold 1997, Cooper, Tajbakhsh et al. 1999, Zammit, Heslop et al. 2002). MyoD upregulation relates to SC proliferation, and SC differentiation depends on MyoD downregulation. MyoD-null mice have shown a limited regenerative capacity characterized by abnormal myoblasts morphology (Sabourin, Girgis-Gabardo et al. 1999) and a decrease in regenerating myofibers (Megeney, Kablar et al. 1996). When SCs enter the differentiation phase, Myogenin and Myf 6 are highly expressed (Grounds, Garrett et al. 1992, Cornelison, Olwin et al. 2000). Myogenin is essential for the fusion of myoblasts either themselves or with existing myofibers. These small myofibers become mature fibers as increasing in size

and express contractile protein such as actin and myosin. On the other hand, Myogenin-null mice have only a few myofibers at birth, and they die prenatally (Hasty, Bradley et al. 1993, Nabeshima, Hanaoka et al. 1993, Venuti, Morris et al. 1995).

The probability of SC transplantation for muscle regenerative medicine has been extensively studied. Donor cells derived myofibers are investigated by donor gene expression in host tissues (Collins, Olsen et al. 2005, Montarras, Morgan et al. 2005). Donor SCs not only fuse with themselves or host myofibers, but also exist as SCs within regenerating myofibers through self-renewal (Collins, Zammit et al. 2007, Sacco, Doyonnas et al. 2008).

Myofibers as a source of satellite cell

SCs are primary sources to contribute skeletal muscle regeneration. Enzymatically dissociated SC transplantation has a challenge to resolve skeletal muscle wasting disorders (Mouly, Aamiri et al. 2005, Tedesco, Dellavalle et al. 2010) because enzymatically dissociated and transplanted SCs result in limited muscle regeneration due to limited migration of SC, donor-host histocompatibility, and early death of donor SCs. Individual, freshly isolated single myofiber transplantation is an alternative way to deliver SCs to damaged muscles. SC delivery through individual single fiber transplantation keeps SC stemness because SCs are influenced by the original environment which increases survival ratio of donor SCs. Individual myofiber contains 7-22 of SCs in a mouse (Seale, Sabourin et al. 2000, Zammit, Heslop et al. 2002), and SCs migrate from the fiber to the damaged site. Single myofiber containing 7 SCs generated more than 100 new fibers containing 25,000-30,000 myonuclei (Collins, Olsen et al. 2005). A single donor myofiber promotes muscle

hypertrophy as well as an increase in CSA (Boldrin and Morgan 2013). Single myofiber transplantation not only results in hypertrophy with high force production, but also donor fiber derived SCs in young age remain in a host muscle permanently which prevents age-related mass reduction (Hall, Banks et al. 2010). A previous study in our lab, transplanting 50 myofibers into pre-embedded ECM results in an increase in the number of regenerating fiber and a decrease in decellularized area in a VML rat.

Resistance training and regeneration

Resistance training (RT) influences on the functional properties in skeletal muscles by modifying fiber structure, mass, metabolism and promoting the release of growth factors. The intensity and mode of exercise induce specific adaptation of skeletal muscles. RT potentially increases muscle mass and contractile properties. After 6 weeks of heavy resistance training, muscle strength increases by 15% (Aagaard, Simonsen et al. 2002). RT enhances muscle protein synthesis ratio in human by 50% at 4 hours after a heavy resistance training (MacDougall, Gibala et al. 1995). RT plays an important role in not only myofiber hypertrophy, but also regenerative capacity (Fry 2004, Folland and Williams 2007). The number of SC increases by 17% after extreme 16 weeks of resistance training (Petrella, Kim et al. 2008). Power lifters containing higher number of SC response to injuries acutely (Thornell, Lindström et al. 2003).

RT is one of the best treatments for VML injury because VML results in severe functional deficits. 10% of the mass of the muscle loss results in 30% of initial peak isometric force reduction (Chen and Walters 2013). When 20% of the mass of the TA is defected, TA exhibits 29 and 31% of a functional deficit in two and four months post-injury

(Corona, Wu et al. 2013). Therefore, VML patients require a special treatment to enhance functional recovery. Low intensity exercise is beneficial to repair of the cardiac tissue (Herdy, Marcehi et al. 2008), and high intensity exercise attracts circulating mesenchymal stem cells in myocardial ischemia patients (Lucia, De La Rosa et al. 2009). Both resistance and endurance training trigger angiogenesis and vascularization (Green, Goreham et al. 1999, Laughlin and Roseguini 2008). This vascularization is a particular concern in repairing or regenerating tissues in order to attract residence and circulating cells. Moreover, Blood vessels provide nutrients and oxygen to support muscle reconstruction (Teixeira, Zamuner et al. 2003).

Innervation and vascularization of the ECM

New myofiber formation should synchronize with vascularization and innervation together because of the role of blood vessels and nerves in skeletal muscles. Transmission of nerve impulses causes skeletal muscle contraction. A nerve fiber consists of axons and myelin sheath is characterized by central nerves and peripheral nerves. Especially, both motor nerve fibers and sensory nerve fibers involving peripheral nerves directly supply muscle contraction. Innervation plays an important role in functional morphological skeletal muscle maintenance (Borisov, Dedkov et al. 2005). Denervated skeletal muscles continue the path of degeneration due to the failure of neuromuscular junctions which results in atrophy and tissue necrosis (Järvinen, Järvinen et al. 2005). Skeletal muscle regeneration occurs following denervation, but this process is not able to continue by SC depletion (Borisov, Dedkov et al. 2005). Since denervation results in adverse effects on the muscle, it is essential that regenerating myofibers should accompany with innervation in a VML injury.

Schann cells, the primary glia of the peripheral nerve fiber, perform nerve regeneration and muscle innervation. Activated Schann cells secrete cytokines and neurotrophic factors that guide axon growth (Shimizu, Kitada et al. 2007). Innervation by axons depends on the remaining Schann cell tubes, as well as Schwann cell extension processes leading to end plates (Son and Thompson 1995). The presence of motoneurons affects Schann cell viability. Motor neurons secrete neuregulins, glial growth factors, that promotes survival and proliferation of Schann cell (Trachtenberg and Thompson 1996, Kopp, Trachtenberg et al. 1997). The effects of neuregulin on muscle by binding tyrosine kinase receptors have been observed. Human myoblasts cultured with neuregulin express an increase in acetylcholine receptors and myosin heavy chains (Jacobson, Duggan et al. 2004). Other studies have researched the role of neurotrophic factors such as nerve growth factor (NGF), neurotrophin-3(NT-3), and brain-derived neurotrophic factor (BDNF) on skeletal muscle regeneration. NGF is important for the survival and growth of neuron. Phenotypic characterization of NGF knockout mice increases in cell death and muscle dystrophy (Ruberti, Capsoni et al. 2000). NGF treated with laminin and Muscle-derived stem cells enhances neurite extension and the engraftment efficiency respectively (Yu, Dillon et al. 1999, Lavasani, Lu et al. 2006). NT-3, a neurotrophic factor, encouraging the growth of the nerve modulates neurogenesis. Transgenic mice for NT-3 overexpression increase the number of sensory and motor neuron, and NT-3 delivery enhances axonal regeneration in denervated muscle (Taylor, Vancura et al. 2001). BDNF supports the survival of existing neurons and promotes growth and differentiation of new neurons (Acheson, Conover et al. 1995, Huang and Reichardt 2001). BDNF also influences on skeletal muscle regeneration. BDNF depleted mice display a decrease in Pax7 positive cells, as well as impair skeletal muscle regeneration. These studies highlight the interaction between nerve growth and

skeletal muscle cells in skeletal muscle regeneration.

Blood vessels supply nutrients and oxygen to muscle tissues. The diffusion distance of oxygen and nutrients from micro vessels to cells is only limited to 150-200 μm (Carmeliet and Jain 2000). Even though immediate hypoxia condition triggers endothelial cell proliferation (KIEFER, BERNIS et al. 2002), muscle tissue are not able to survive without blood supply in a long term. Endothelial cell (EC)s located the interior surface of blood vessels are involved in vascular biology. EC transplantation in myocardial injury stimulates angiogenesis which results in an increase in regional perfusion (Kim, Kwon et al. 2001). Vascular endothelial growth factor (VEGF) is a primary regulator of angiogenesis. VEGF derived angiogenesis promotes skeletal muscle regeneration. VEGF overexpression via virus gene transfer shows an increase in forelimb strength and an decrease in necrotic fibers area in mdx mouse (Messina, Mazzeo et al. 2007). Combined delivery of VEGF and IGF-1 led to angiogenesis, innervation, and SC activation which results in functional recovery (Borselli, Storrie et al. 2010). In a previous research in our lab, transplantation of mesenchymal stem cells into acellular ECM increases blood vessel density which results in functional recovery.

Significance

Skeletal muscles have an ability to heal in general injuries, but skeletal muscles are not capable of regenerating across a large gap. The repercussions of this severe injury cause subsequent functional deficits due to loss of nerves, vessels and muscle mass. Moreover, people who sustain VML injury suffer from emotional distress by physical abnormalities and aesthetic deficits. Physical and psychological rehabilitative processes cost large amount of money. General current clinical treatments transplanting only biocompatible matrix or autologous acellular ECM have not yet completed functional and morphological recovery. Preliminary researches in our lab showed the probability of functional and morphological recovery in a VML rat with mesenchymal stem cells (Merritt, Cannon et al. 2010) and nerve relocation treatments (Tierney et al., 2010, unpublished), but still lots of fibrotic tissues exist within ECM, and mechanical properties are not fully recovered. SC transplantation for skeletal muscle regeneration is a very commonly researched treatment. Delivery of SC through single myofiber has shown functional recovery and hypertrophy in mdx mice not a naïve animal model (Collins, Olsen et al. 2005; Hall, Banks et al. 2010; Boldrin and Morgan 2013). Resistance training is a well-known treatment to trigger hypertrophy and an increase in muscle mass, but the potential interaction between resistance training and muscle cell activation should be studied. Therefore, the findings in this study will suggest the therapeutic potential of a VML injury with myofiber transplantation and resistance training.

Method

Animals

Male Fisher 344 rats (Charles River Laboratories; Wilmington, MA), about 400g of weight, were used in this study. F344-Tg (UBC-EGFP) was used for a myofiber donor. Animals were housed on a 12 hour light/dark cycle room and given ad-libitum access to food and water. Rats were randomly assigned to one of four groups (n=8). Rats were evaluated functionally after 56 days of recovery from initial defect surgery. All experimental procedures were conducted in accordance with guidelines set by Institutional Animal Care and Use Committee (IACUC).

ECM decellularization

Extracellular matrices from the porcine decellularized in a method similar to Merritt, but with modifications (Merritt, Cannon et al. 2010). Fat and connective tissues were excised from muscles and cut into small pieces. Deionized water (dH₂O) was injected throughout the whole muscles and the muscles placed in dH₂O for 2 hours to allow for cellular swelling and rupture. PBS was injected throughout the entire muscles, and the muscles were placed in PBS for 2 hours. 0.25% Trypsin-EDTA(Gibco[®] Life Technologies,) was injected throughout the entire muscles, and the muscles were placed in an oven for 45 minutes at 37°C. The tissues were then placed in a glycerol (Fisher; Pittsburgh, PA), disodium ethylenediaminetetraacetate dehydrate (EDTA) (Bio-Rad Laboratories; Hercules, CA), deoxycholic acid (Fisher; Pittsburgh, PA), and sodium dodecyl sulfate (SDS) (Sigma-Aldrich; St. Louis, MO) solution for 48 hours. The tissues were run in the electrophoresis

machine with Tris base (Fisher; Pittsburgh, PA), Glycine (Fisher; Pittsburgh, PA), and SDS (Sigma-Aldrich; St. Louis, MO) solution at a constant voltage of 60V for 24 hours. 2% SDS was injected through the muscles, and then the muscles were placed in SDS for 6 hours. The electrophoresis process was repeated until all cellular materials were eliminated. The ECM was rinsed in dH₂O until water looked clear. The ECM was placed in sterile phosphate buffered saline (Invitrogen; Carlsbad, CA) 1% antibiotic-antimycotic (Sigma-Aldrich; St. Louis, MO) (1% AA) overnight on a shaker. Next, the ECM was placed in 70% ethanol for 4 hours, subsequently placed in PBS 1% AA and exposed to ultraviolet light overnight. Decellularized ECMs were stored at 4°C in sterile PBS with 1% AA until use in implantation.

VML creation & ECM implantation

Prior to VML surgery, all animals were randomly assigned to one of four experimental groups: implantation of the ECM (ECM), implantation of the ECM followed by myofiber injection (FIB), implantation of the ECM followed by resistance training (EXE), and implantation of the ECM followed by myofiber injection and resistance training (FIB+EXE). All animals underwent removal of about 20% of muscle mass from the lateral gastrocnemius (LGAS). A piece of the same dimensions of ECM was transplanted immediately, and myofibers were injected seven days later as described by Collins (Collins, Olsen et al. 2005). All surgeries were conducted with aseptic tools while rats were anesthetized with 2-2.5% isoflurane gas.

Briefly, a two-centimeter incision was made along the lateral side of the right lower leg, parallel with the tibia. The lateral portion of the LGAS was exposed by separating the

biceps femoris. The soleus was gently separated from the LGAS by blunt forceps. A metal plate was placed between the soleus and the LGAS to prevent injury to the soleus upon creation of LGAS defect. Two #9 scalpel blades separated 1 cm by a spacer was used to create the equal shape of defect to all animals. Approximately, 1.0 x 1.0 cm full thickness with 20% of mass of the LGAS was excised. Immediately following defect, an ECM was prepared to the same dimension of the excised muscle and implanted to the site of injury using a nonabsorbable 5-0 polypropylene (5-0 prolene; Ethicon) suture. The ECM was fixed with A modified Kessler's stitch with simple interrupted sutures on three borders. The sutures were used as markers to distinguish between original tissues and regenerating tissues for histological and immunohistological analysis (Kragh Jr, Svoboda et al. 2005). The biceps femoris was closed using simple interrupted polypropylene sutures (5-0 prolene; Ethicon). The skin was sutured via a simple interrupted suture (5-0 prolene; Ethicon) with the knot tied underneath the skin.

Myofiber isolation

EDL was digested by filtered 1.5% Collagenase type I in DMEM for 2 hours at 37°C and 5% CO₂. During digestion EDL was gently shook every 30 minutes. When single myofiber detaches from the EDL, EDL and single fiber were transferred to a prewarmed Petri dish with DMEM. Single myofiber was isolated by pipetting.

Treatment surgery

Myofiber injection animals underwent 7 days recovery to mitigate inflammation and

increase the survival ratio of injected fibers. The original stitches were removed to expose and visualize the ECM. GFP-myofibers were isolated from F344-Tg (UBC-EGFP). 30 myofibers were injected evenly though the entire injury area using a 28.5-gauge needle with saline (SAL). After fiber injection, the biceps femoris and skin were sutured as previously described.

Exercise protocol

Exercise treatments groups, EXE and FIB-EXE, began resistance training at 7 days post defect surgery. This time was given to allow for ECM adhesion with the injury site and force transmission across the defect (Kjær 2004). Rats were subjected to climb a ladder every third day for 6 weeks. The ladder was 1-m height with 2-cm steps and inclined at 85% degree. Rats were familiarized with the ladder by climbing the ladder three times for three days before a surgery. The weights were attached to the proximal tail, and the initial weight attached to a rat was 50% of body weight. The animals were encouraged to climb the ladder by gently touching the tail and pushing the behind. When rats completed climbing the ladder, they were allowed to take 2 minutes rest in a simulated cage at the top of the ladder apparatus. The load was set at 50, 75, 90, and 100% of maximum load from the previous session. When a rat was able to climb with 100% of maximum load, 30g of weight was added subsequently until the rat failed to climb the ladder.

Functional analysis

All rats had a 56 day of recovery time and underwent *in situ* functional measurement

on both contralateral and experimental legs. Animals were anesthetized as previously described, and both legs were shaved. A skin incision was created 2-cm below and parallel to the femur to expose a sciatic nerve. The sciatic nerve was severed as close as possible to the hip to secure an enough length for an electrical stimulation. A longitudinal skin incision was created at the posterior portion of the leg from the calcaneus to the head of gastrocnemius (GAS). A biceps femoris incision was made like a skin incision from the calcaneus to the head of gastrocnemius. A nerve branch for medial gastrocnemius was cut to allow only force generation from LGAS. The calcaneus was cut with the Achilles tendon to separate the GAS from the tibia. Plantaris and soleus were separated from the GAS to ensure that the LGAS was an only subject to contribute to force production. A 1/16th inch drill bit was penetrated the posterior portion of the tibia head to fix GAS head. The Achilles tendon tied to the level arm (model 310-B, Aurora Scientific, ON, Canada). The severed sciatic nerve was placed on electrodes and stimulated by a stimulator (Model 2100; A-M Systems, Carlsborg, WA). Mineral oil was used to prevent the LGAS and sciatic nerve from drying and a heat lamp was used to maintain the muscle temperature between 36.5 and 37.5°C. Optimal length was set and maximal tetanic contraction was measured at 150Hz and the minimal voltage to elicit maximal tetanic contraction. Tetanic contraction was separated by 2 minutes of rest. The process was applied to the contralateral leg. After force measurement was completed, the LGAS and MGAS were excised, weighted, and measured a length to calculated specific tension. All muscles were frozen in liquid nitrogen and stored at -80°C.

Histology analysis

LGAS were sectioned into 10 μm sections perpendicular to the LGAS orientation with a Leica CM1900 cryostat microtome (Leica Microsystems; Wetzlar, Germany) at -20°C . Hematoxylin and eosin (H&E) (Thermo Fisher Scientific) staining were performed to identify intact fibers and regenerating fibers. Masson's trichrome (Polyscience) was used to define myofiber and fibrous connective tissue area. Sections were mounted with permount mounting medium (Fisher Scientific; Waltham, MA). Sections were visualized with a Nikon Diaphot microscope with an Optronix Microfire digital camera. Histological quantification of H&E was performed on each level with the 20x objective lens.

Immunohistochemical analysis

Series of 10 μm cross sections were taken from top, middle and bottom regions of the LGAS muscle. In preparation for immunofluorescent identification, sections were fixed in acetone for 3 minutes. After which, they were washed in phosphate buffered saline (1X, PBS) and blocked with 5% normal donkey serum in PBS containing 1% bovine serum albumin (BSA). Sections were first incubated with primary antibodies against PECAM-1 (1:20, mouse monoclonal) and neurofilament 200 (1:200, rabbit polyclonal). PECAM-1 was detected with donkey anti-mouse IgGTRITC fluorescein (1:100, $\lambda=546\text{ nm}$) and neurofilament 200 was detected with anti-rabbit-Alexa 488 (1:100, $\lambda=495\text{ nm}$). Finally, all sections were counterstained with DAPI (1:1000, $\lambda=425\text{ nm}$) to identify nuclei. Following a final series of washes in PBS, sections were mounted in Permount mounting medium (Fisher Scientific; Waltham, MA).

Imaging and analysis

Immunofluorescence was visualized with a Leica DM LB2 fluorescence microscope and photographed with a Leica DFC340FX digital camera (Leica Microsystems; Wetzlar, Germany). At each level and within each region of the ECM, the number of nerve and vessels was counted using Image J and expressed as a percentage of the total number of blood vessels and nerves in the ECM area. 24 vessels were counted in each image and expressed as the number of blood vessels present per unit area of the ECM (#/mm²). A vessel was only counted if its lumen was greater than 20 μ m in diameter.

Statistical analysis

Data has been represented as mean \pm SEM. One-way ANOVA was used for analysis of group samples. Comparisons between groups made using Tukey's post hoc tests. Statistical significance is defined as $p < 0.05$.

Result

The average mass of the removed muscle was 176 ± 16 mg wet weight approximately 20 % of the total mass of the LGAS, the defect mass was approximated by body weight. Overall morphology of the LGAS was flat on defected side compared to a contralateral limb. Previous work in our lab using homologous ECM transplantation, the morphology of the LGAS was well maintained following 56 day recovery (Merritt, Cannon et al. 2010), but transplantation of porcine ECM was not maintained original round shape. The sum of the injured LGAS mass and originally removed muscle mass was $99.4\% \pm 1.7\%$ of the mass of the contralateral LGAS.

Histological analysis following 56 days of recovery demonstrated small myofiber growth within the ECM and regenerating fibers with central nuclei (Figure 3). Both small myofibers and myofibers containing central nuclei mean these fibers are in the processes of regenerating and maturing. Especially, a large size of myofiber with central nuclei was located at the border between the ECM and intact muscles (Figure 3). CSA was measured in uninjured area to investigate compensatory hypertrophy and resistance training effect (figure 4). EXE group ($5122 \pm 92 \mu\text{m}^2$) increased CSA significantly compared to ECM ($4668 \pm 79 \mu\text{m}^2$), FIB ($4795 \pm 82 \mu\text{m}^2$), and FIB+EXE ($47642 \pm 97 \mu\text{m}^2$) groups (Figure 5).

Immunohistochemical analysis showed neurogenesis and angiogenesis of the ECM. Neurofilament staining revealed the presence of innervation at regenerating area filled with central nuclei myofibers (Figure 6). However, nerves were not detected in the middle or peripheral of the ECM where no mature fibers exist. Quantification of total number of nerves through in the entire area showed no significant differences between groups (Figure 7A). Nerve CSA was measured and evaluated by size distribution. Small size of nerves less than

1000 μm^2 was dominant in all groups. PECAM staining showed angiogenesis at regenerating area filled with central nuclei myofibers, and in the middle of ECM filled with small myofibers and fibrotic tissues (Figure 8). Quantification of the number of blood vessel larger than 20 μm in the entire area showed a significant difference in EXE group (46 ± 4.2) compared to ECM group (35 ± 3.89) (Figure 9 A). EXE group (34 ± 3.2) significantly increased the number of blood vessel in regenerating area compared to ECM group (22 ± 3.3).

In previous research in our lab, the middle region of ECM did not repair well than top and bottom regions. Fibrous connective tissues were measured by Masson's trichrome staining. A significant difference in connective tissue area in middle region of the ECM was quantified between EXE ($45\pm1.6\%$) and ECM ($69\pm1.9\%$) groups (Figure 10). Moreover, small muscle fiber area within ECM was significantly higher in EXE group ($1.39\pm0.15\ \mu\text{m}^2$) than ECM and FIB groups ($0.67\pm0.15\ \mu\text{m}^2$) (Figure 11). Although EXE group tended towards a higher number of blood vessel and nerve compared to other groups, this difference was not significant (Figure 12).

Discussion

The large volume of skeletal muscle loss usually results in functional deficits, cosmetic flaws, and a permanent handicap. Associated psychological distress ensues from functional deficits and cosmetic flows accompanied with traumatic injuries. Current therapies can improve myofiber infiltration and functional properties, but fail to limit fibrosis and fail to improve angiogenesis and myofiber infiltration into middle region of the ECM. Therefore, it is imperative to develop a therapy that is able to improve myofiber infiltration through entire regions in ECM.

This study tested whether the combined effect of myofiber injection and resistance training on a VML injury. The results show only EXE group produces positive effects on skeletal muscle regeneration after 8 weeks of recovery. EXE group increases 15.7% of mass recovery significantly compared to DEF group. RT potentially increases muscle protein synthesis ratio, muscle mass, and contractile properties. Ladder climbing training has resulted in a 5–26% increase in muscle mass (Ho, Roy et al. 1980, Duncan, Williams et al. 1998, Hornberger Jr and Farrar 2004). Several muscle groups can be affected by ladder climbing including the soleus, plantaris, and gastrocnemius (Ho, Roy et al. 1980, Duncan, Williams et al. 1998, Hornberger Jr and Farrar 2004). In previous research in our lab, 8 weeks of ladder climbing increases 23% of mass and 14% of tetanic tension in flexor hallucis longus muscle (Lee, Barton et al. 2004). Moreover, muscle hypertrophy induced 6 weeks of ladder climbing in VML injured LGAS results in 11% of mass and 16% of functional recovery more than only ECM treated group (Taejeong Song et al. 2015, unpublished).

Transmission of nerve impulses causes skeletal muscle contraction. Innervation plays an important role in functional morphological skeletal muscle maintenance (Borisov, Dedkov

et al. 2005). Since denervation results in adverse effects on the muscle, it is essential that regenerating muscle fibers should accompany with innervation in a VML injury. A 12-week high resistance training has a slowly progressive effect on neuromuscular diseases (Kilmer, McCrory et al. 1994). Resistance exercise induces a robust elevation of circulating BDNF (Yarrow, White et al. 2010). Previous studies in our lab reveal that the ECM can provide a room to support cellular myofiber, and blood vessel growth, therefore we postulate that resistance training triggers innervation into ECM. In this experiment, EXE and FIB+EXE groups tend to have higher number of nerve, but the difference is not significant. Innervation only occurs regenerating area containing mature size of myofiber. Neurofilament staining does not detect nerve like-structures with in ECM containing small myofibers or connective tissues. The innervation is the last step in skeletal muscle regeneration process that affect myofiber maturation and functional recovery (Musrò 2014). This study shows that ECM constructs have the capability of allowing innervation as muscle tissues become mature.

Blood vessels supply nutrients and oxygen to muscle tissues. In a previous research in our lab, transplantation of ECM alone or with mesenchymal stem cells increases blood vessel density. It means that the transplanted ECM is able to process angiogenesis. In this study, EXE group contains significantly higher number of blood vessel than ECM group in both regenerating area and entire area. Resistance and endurance training trigger angiogenesis and vascularization (Green, Goreham et al. 1999; Laughlin and Roseguini 2008). Exercise training has been showed an increase in capillary density by VEGF (Amaral, Papanek et al. 2001) and endothelial progenitor cells (Laufs, Werner et al. 2004). Resistance training also increase capillaries per fiber (McCall, Byrnes et al. 1996).

The remarkable founding in this study is that EXE group results in a decrease in

fibrosis and an increase in regenerating small muscle fibers in a middle region of the ECM. A repair of VML injury with an only ECM implantation results in deficient recovery associated functional loss and insufficient myofiber infiltration into middle region of ECM (Merritt, Hammers et al. 2010). Although the implanted ECM bridges the gap, the infiltrating myofibers and blood vessels are limited to top and bottom regions which are close to uninjured muscle. RT influences on the remodeling of ECM, and RT is effective SC proliferation (Darr and Schultz 1987, Mackey, Esmarck et al. 2007). Continuous RT in every three days keeps triggering proliferation of SC, which helps myofiber infiltration into the middle region of the ECM.

The combined treatments do not have an additive effect. Even though the significant difference does not find between EXE and EXE+INJ group, EXE group tend to recover more LGAS muscle mass. EXE group recover 87.6% of LGAS mass while EXE+INJ groups recover only 75.2% of LGAS mass. After 6 weeks of resistance training EXE group climb the ladder with 227% of body mass while EXE+INJ group climb the latter with 187% of body mass. EXE group significantly lifts more weight compared to EXE+INJ group. EXE+INJ receives surgeries twice, a defect surgery and a surgery for fiber injection, which may trigger additional damage.

In summary, this study proves that the treatment of a VML injury with continuous RT following ECM implantation significantly effects on histological and morphological recovery over ECM implantation alone. Future studies may combine resistance training with MSC to examine the additive effect. Also, long term resistance training need to be examined because 56 day of recovery time does not seem enough to complete of muscle regeneration in 20% mass of VML injury. Small myofibers are still growing in entire region of the ECM.

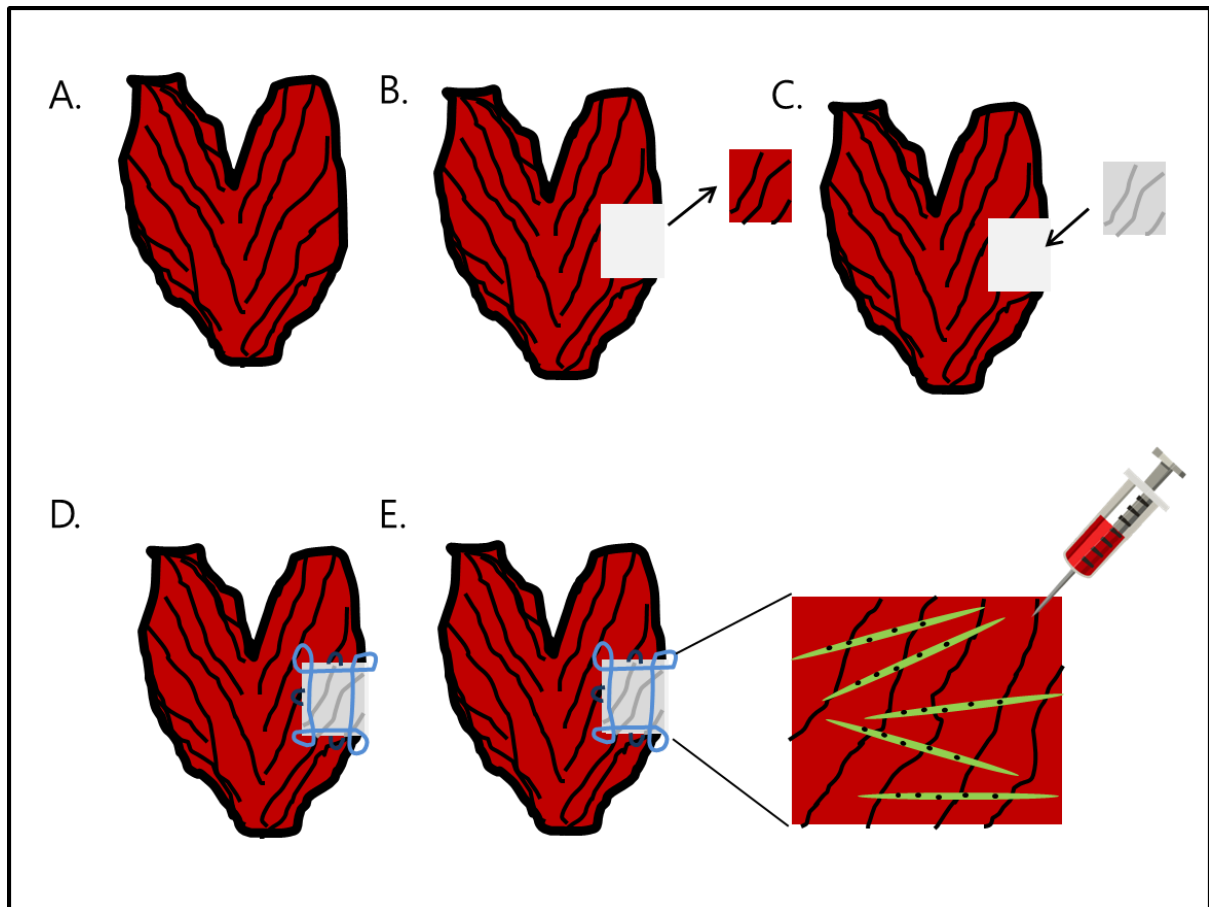


Figure 1: Schematic diagram of surgical procedures in VML injury model.

Uninjured LGAS. B.) Creation of 1x1cm VML injury. C.) ECM transplantation. D.) Mark injury area by using a modified Kessler stitch. E.) Injection of GFP single myofiber, 7 days post injury.

Day	Procedure	Day	Procedure
-3	Familiarization	28	
-2	Familiarization	29	Lift 7
-1	Familiarization	30	
1	Defect Surgery	31	
2		32	Lift 8
3		33	
4		34	
5		35	Lift 9
6		36	
7		37	
8	Fiber Injection	38	Lift 10
9		39	
10		40	
11	Lift 1	41	Lift 11
12		42	
13		43	
14	Lift 2	44	Lift 12
15		45	
16		46	
17	Lift 3	47	Lift 13
18		48	
19		49	
20	Lift 4	50	Lift 14
21		51	
22		52	
23	Lift 5	53	Lift 15
24		54	
25		55	Lift 16
26	Lift 6	56	Force Measures and Sacrifice
27			

Figure 2: Surgery and Treatment schedule

1. Entire Region

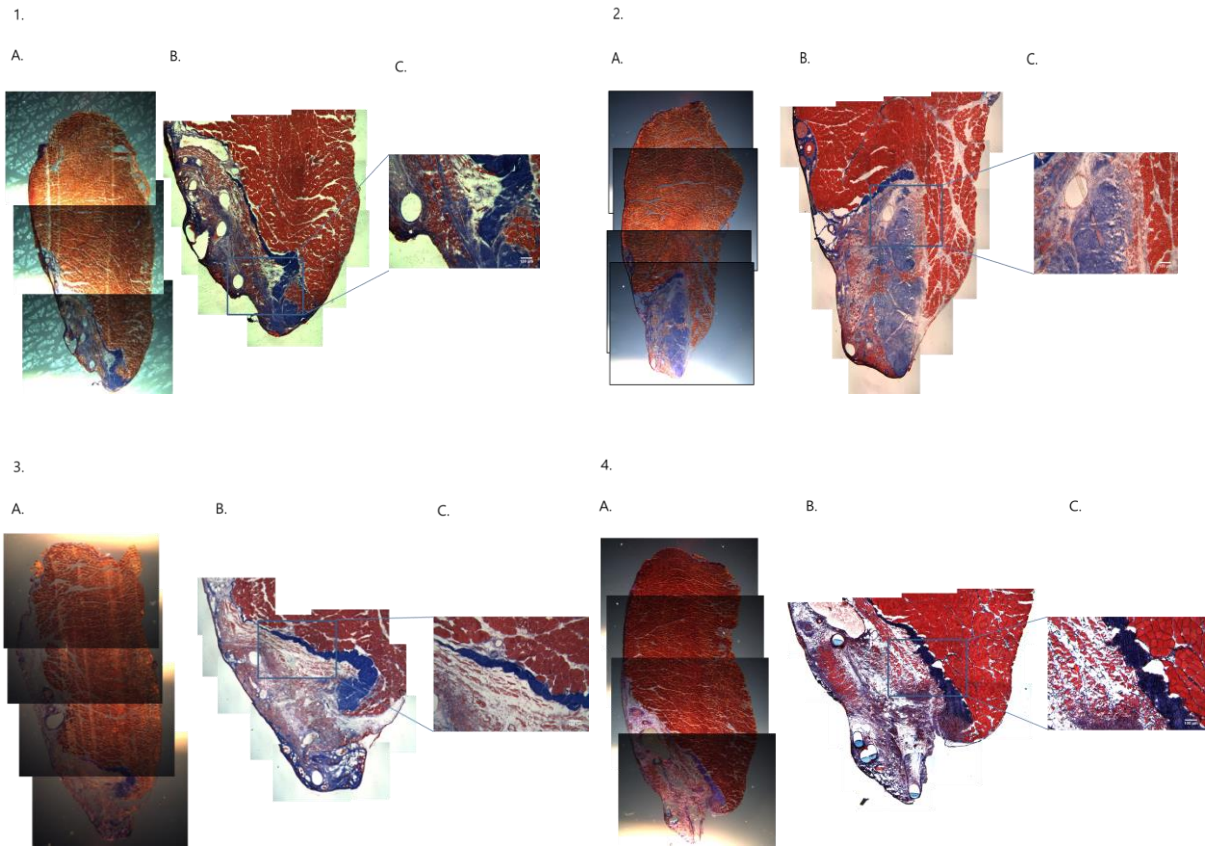


Figure 3: Masson's trichrome staining. Sections showing myofiber infiltration and fibrotic tissue growth in implanted ECM taken with 2.5x, 5x, and 10x objective lens. (1.) ECM. (2.) FIB. (3.) EXE. (4.) FIB+EXE. A.) Entire muscle B.) Regenerating muscle C.) Regenerating muscle. Scale bar = 100 μm .

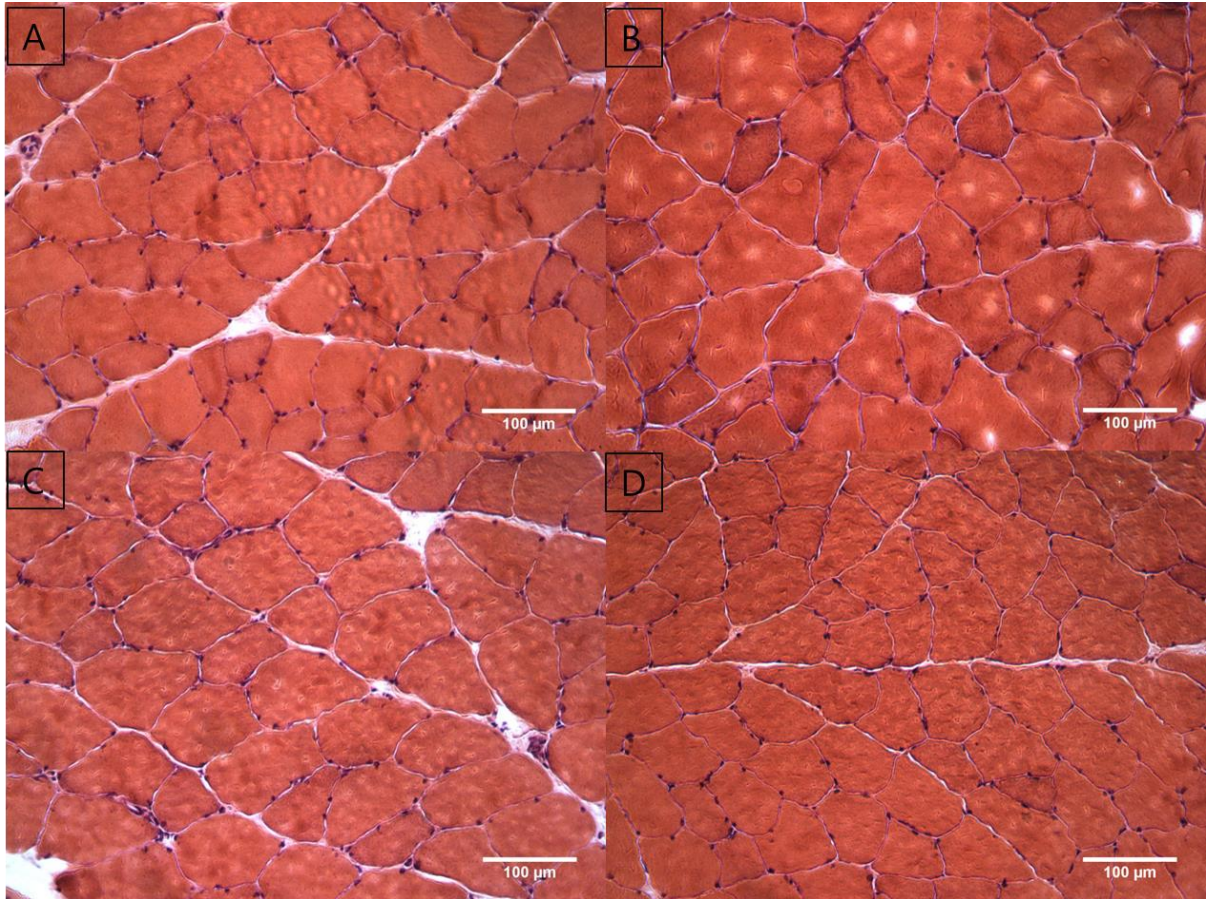


Figure 4: Hematoxylin and eosin staining. H&E sections showing intact muscle CSA hypertrophy in EXE group (A.) ECM. (B.) FIB. (C.) EXE. (D.) FIB+EXE. Scale bar = 100 μm .

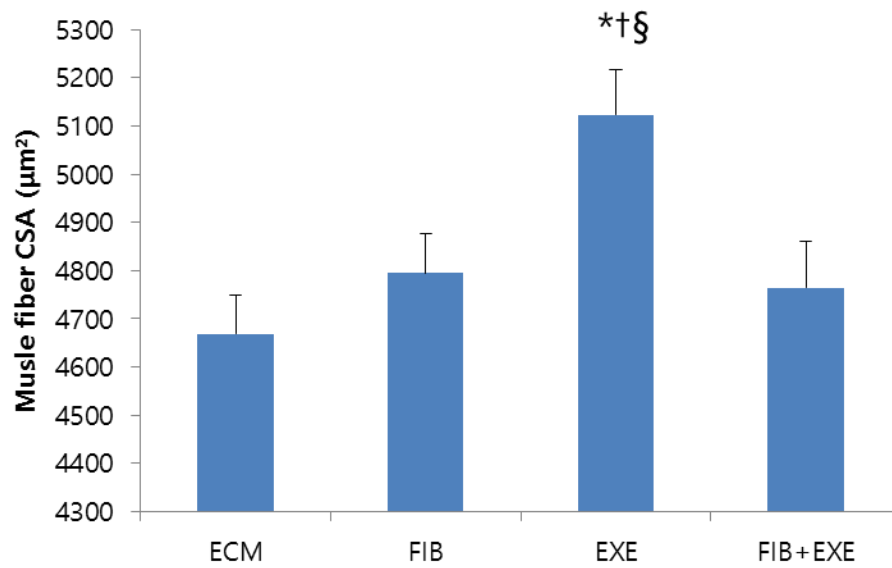


Figure 5: Cross sectional area in uninjured myofiber. CSA was determined through Hematoxylin & Eosin staining. * denotes significant difference compared to ECM. † Denotes significant difference compared to FIB only. ‡ denotes significance compared to EXE group. § denotes significance compared to FIB+EXE Significance is set at $p < 0.05$

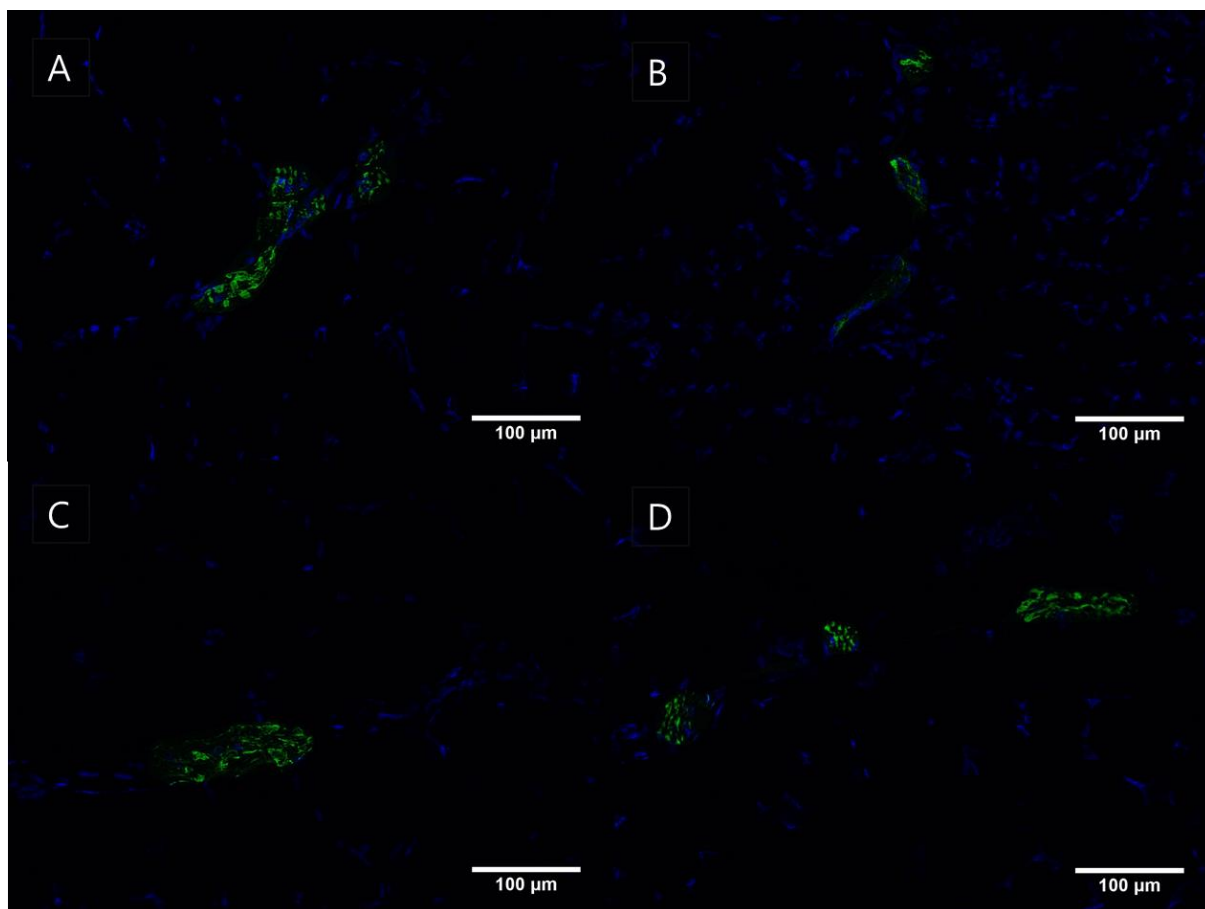


Figure 6: Neurofilament staining. Innervation observed via Neurofilament staining in regenerated muscle area closed to regenerating region, image taken with 20x objective lens. (A.) ECM. (B.) FIB. (C.) EXE. (D.) FIB+EXE Scale bar = 100 µm.

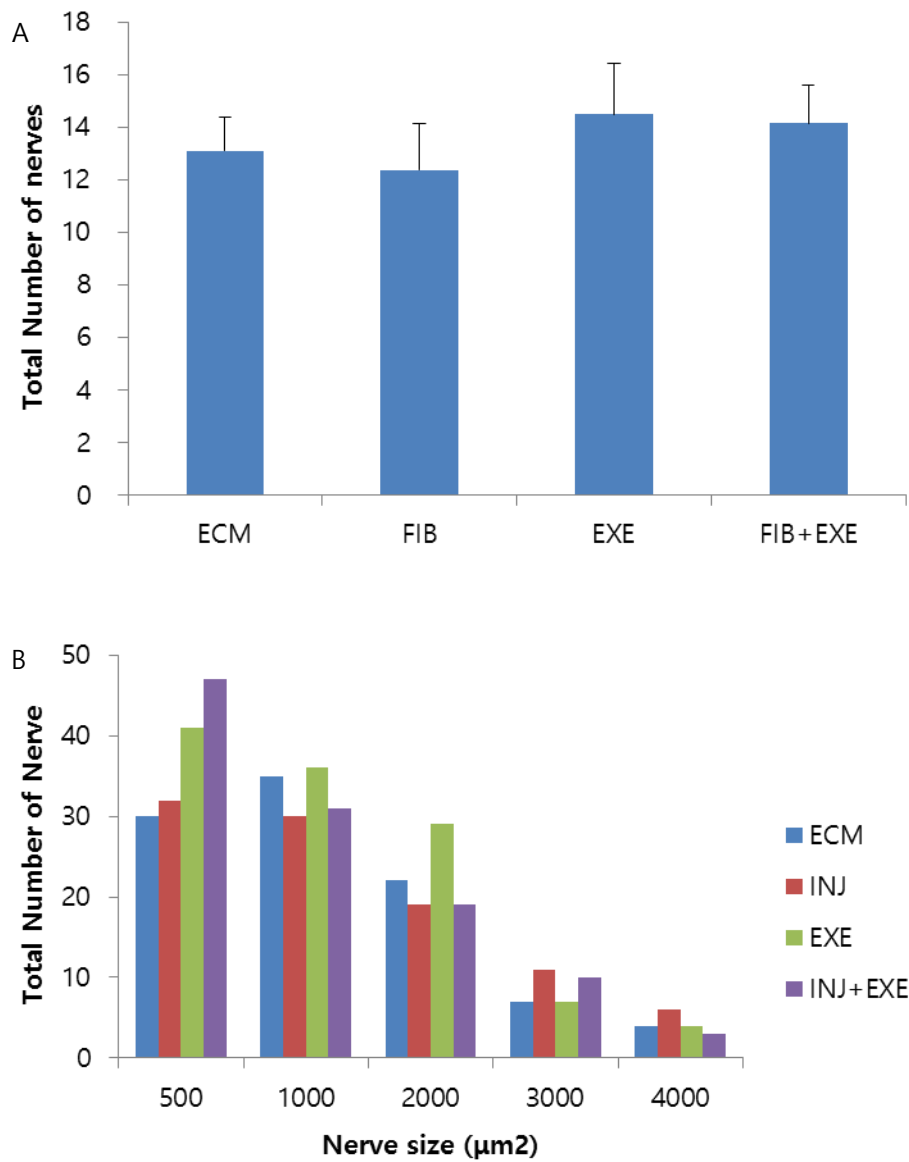


Figure 7: Total number of Nerves and size distribution. A.) Total number of nerves was counted through Neurofilament staining. B.) Nerve size distribution was determined. * denotes significant difference compared to ECM. * denotes significant difference compared to ECM. † Denotes significant difference compared to FIB only. ‡ denotes significance compared to EXE group. § denotes significance compared to FIB+EXE Significance is set at $p < 0.05$

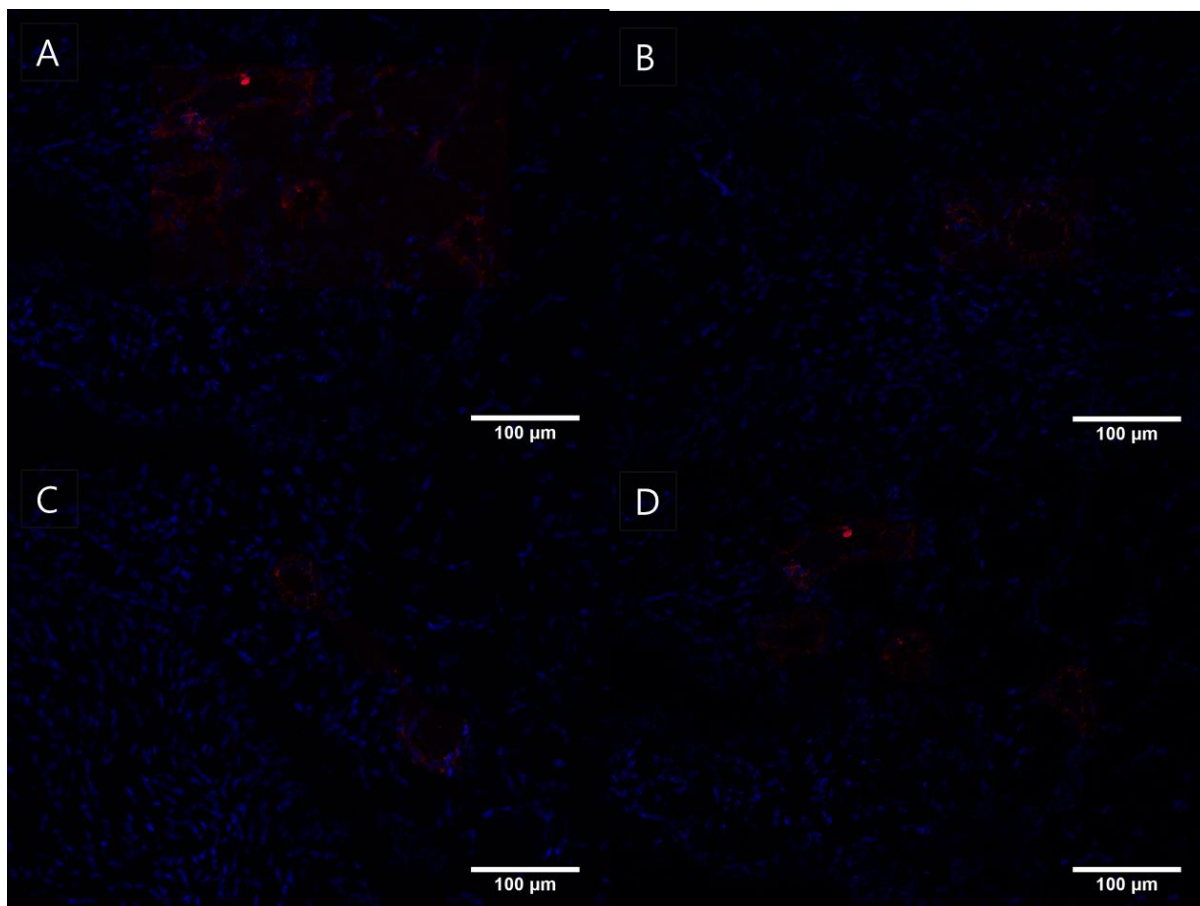


Figure 8: PECAM staining. Angiogenesis observed via PECAM staining in regenerating muscle area, images taken of blood vessels $\geq 20\mu\text{m}$ diameter (A.) ECM. (B.) FIB. (C.) EXE. (D.) FIB+EXE Scale bar = 100 μm .

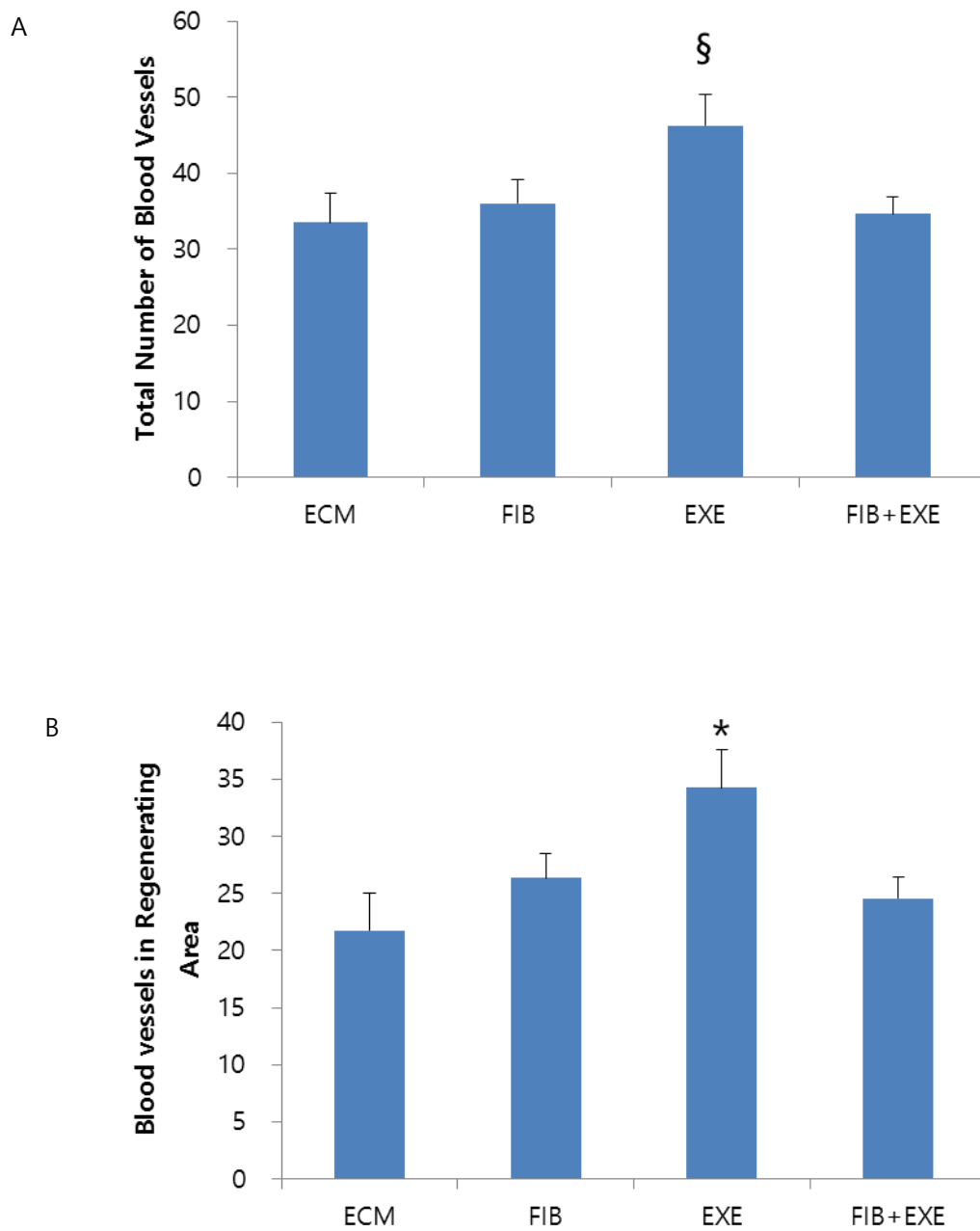


Figure 9: Number of blood vessel. A.) Total number of blood vessel was counted through entire area. B.) Blood vessel number was determined in regenerating muscle area, images taken of blood vessels $\geq 20\mu\text{m}$ diameter. * denotes significant difference compared to ECM. † Denotes significant difference compared to FIB only. ‡ denotes significance compared to EXE group. § denotes significance compared to FIB+EXE Significance is set at $p < 0.05$

2. Middle Region

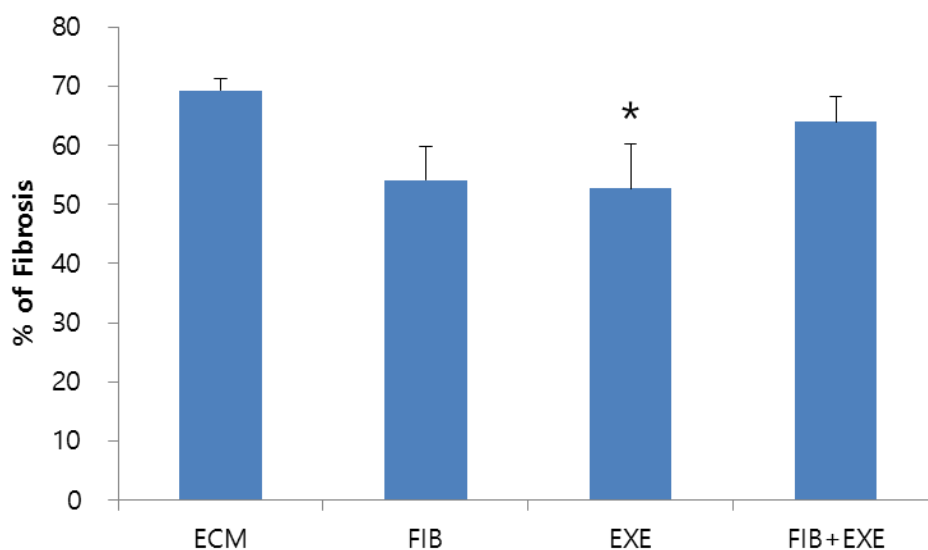


Figure 10: Fibrotic tissue density in Middle region of VML. Fibrosis observed via Masson's trichrome staining in regenerating muscle area. * denotes significant difference compared to ECM. † Denotes significant difference compared to FIB only. ‡ denotes significance compared to EXE group. § denotes significance compared to FIB+EXE. Significance is set at $p < 0.05$

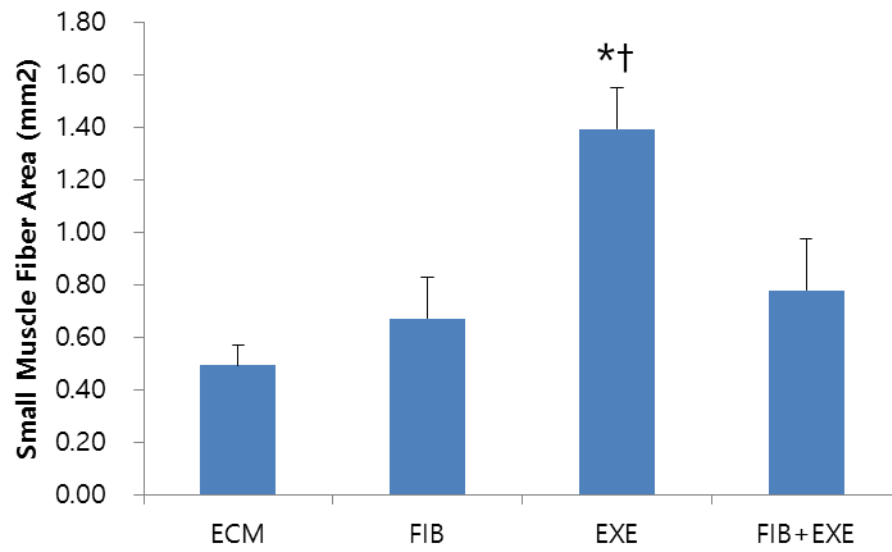


Figure 11: Small myofiber density in Middle region of VML. Myofiber ingrowth was observed in regenerating muscle area. * denotes significant difference compared to ECM. † Denotes significant difference compared to FIB only. ‡ denotes significance compared to EXE group. § denotes significance compared to FIB+EXE Significance is set at $p < 0.05$

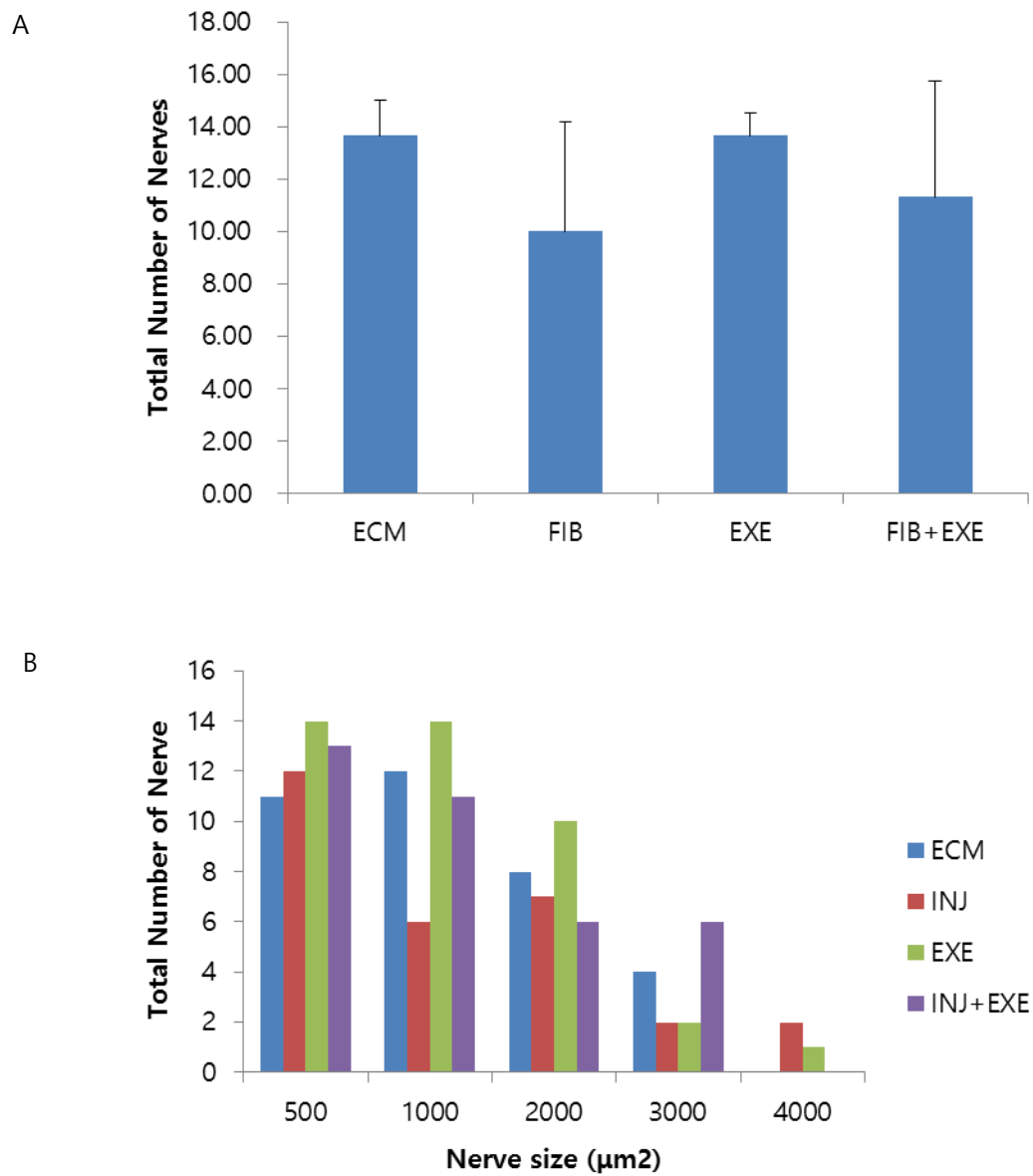


Figure 12: Total number of nerve and size distribution in Middle region of VML. A.)

Total number of nerves was counted through Neurofilament staining. B,) Nerve size distribution was determined. * denotes significant difference compared to ECM. * denotes significant difference compared to ECM. † Denotes significant difference compared to FIB only. ‡ denotes significance compared to EXE group. § denotes significance compared to FIB+EXE Significance is set at $p < 0.05$

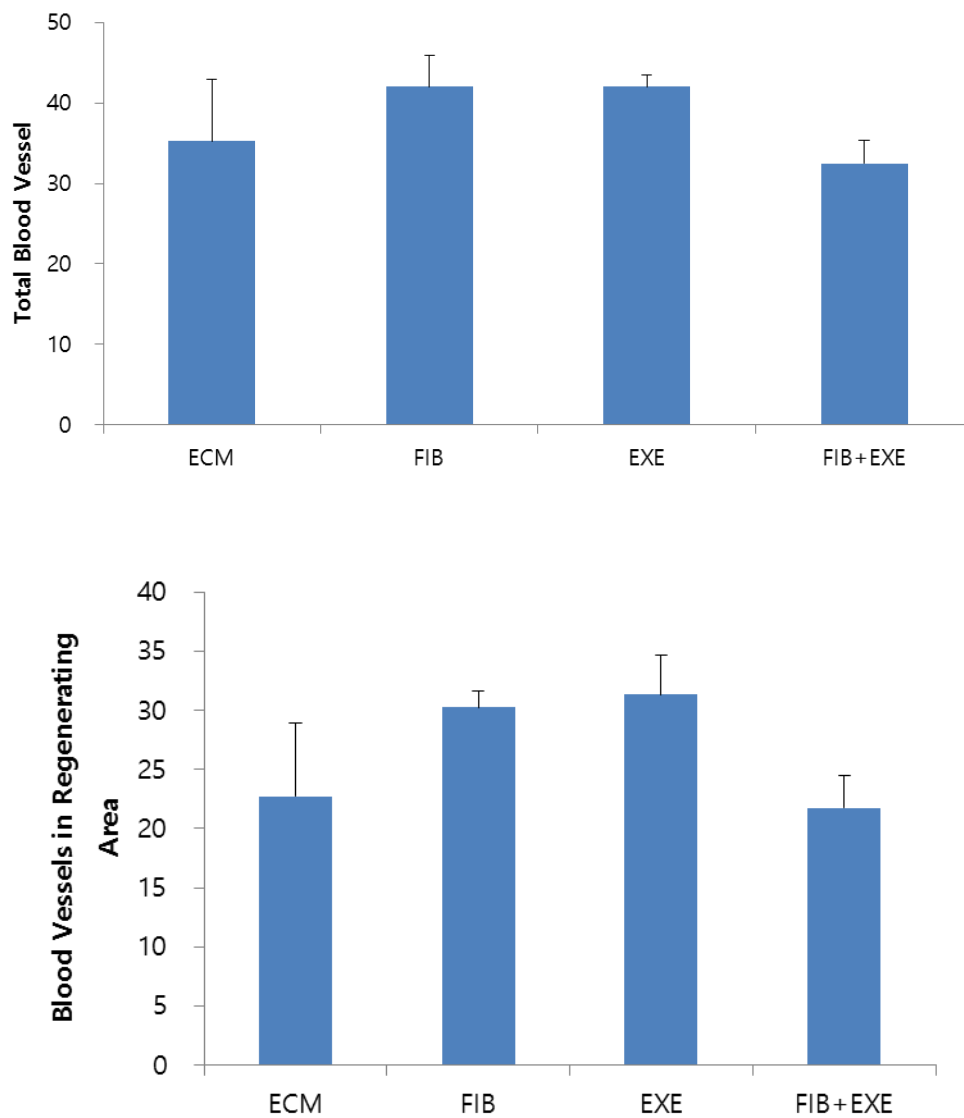


Figure 13: Blood vessel density in Middle region of VML . Blood vessel number was determined in regenerating muscle area, images taken of blood vessels $\geq 20\mu\text{m}$ diameter. * denotes significant difference compared to ECM. † Denotes significant difference compared to FIB only. ‡ denotes significance compared to EXE group. § denotes significance compared to FIB+EXE Significance is set at $p < 0.05$

Appendix A: Expended Methods

I .Extracellular matrix decellularization

1. Remove connective tissue and fat from porcine tissue, and cut into smaller pieces.
2. Inject dH₂O throughout the entire tissue, and leave in a dH₂O filled container for 2 hours, and place on an orbital shaker.
3. Discard dH₂O, Inject dH₂O throughout the entire tissue, and leave in a dH₂O filled container for 2 hours, and place on an orbital shaker.
4. Discard PBS, inject trypsin throughout the whole tissue, fill a container with enough trypsin to immerse the tissue, and place in oven for 45 mins at 37°C.
5. Discard trypsin, and fill in PBS for 2 hrs
6. Discard PBS, inject glycerol solution throughout the entire tissue, and place in a container with enough glycerol.
7. Place on shaker for 48 hrs at room temperature. It is able to keep at 4°C for a long time)
8. Discard glycerol, and wash with dH₂O
9. Run in an electrophoresis machine with tris-glycine solution at 60V for 24 hrs.
10. After running electrophoresis, inject 2% SDS throughout the tissue, and place in 2% SDS on an orbital shaker for at least 6hrs.
11. Change the tris-glycine solution before running electrophoresis again.
12. Repeat steps 9-11 until muscle looks clear.

13. Store cleared tissues in 2% SDS.
14. Rinse in dH₂O again, repeat several times until water looks clear.
15. Place tissues in PBS with 1% AA overnight on a shaker.
16. Place tissues in 70% ethanol for 4 hours.
17. Place tissues in PBS with 1% AA overnight under UV light.

II. Volumetric Muscle Loss Surgery:

1. Before starting surgery, autoclave all surgical instruments that will directly contact the animal.
2. The animal should be observed and recorded in every 15 minutes through entire surgical procedure.
3. Weigh and anesthetize the animal with 2.5% of isoflurane infusion. The animal should exhibit absence of toe pinch reflection and normal breathing.
4. Shave the hindlimb where the defect will be created.
5. Create a 2cm incision with a scalpel on the lateral side of leg, parallel with the tibia.
6. Separate the biceps femoris to expose the LGAS
7. Gently make a space between the LGAS and soleus, and place an aluminum foil plate in which LGAS defect will be created to prevent soleus from injury.
8. Calculate estimated 20% mass of the LGAS by weight.

9. Create 20% mass of the full-thickness defect from distal to the neuromuscular junction by two scalpel blades separated by 1cm spacer.
10. Weigh the excised muscle and create small size of defect until 20% mass is removed.
11. Prepare a same dimension of ECM to the defect and implant it into the defected site.
12. Suture the ECM using a modified Kessler stitch with non-absorbable 5-0 polypropylene sutures.
13. Stitch simple sutures at the borders of the ECM and LGAS to mark the edges of the ECM
14. Suture the biceps femoris using simple interrupted sutures and the skin incision with the knot tied underneath the skin to prevent the animal from biting the knot.
15. Return the animal to a cage and monitor until the animal has recovered consciousness
16. Give subcutaneous analgesic, Rimadyl, .01ml/g at 12 hrs, 24, and 48 post surgery.

III. Single Fiber Isolation:

1. For the purpose of these experiments, 8 week old F344-Tg (UBC-EGFP) were used.
2. Filter 1.5% Collagenase type I in DMEM (Dulbecco's modified Eagle's medium; high glucose, L-glutamine with 110 mg/ml sodium pyruvate) through 0.22 μ m filter.
3. Prewarm a solution at 37 °C in a water bath before the isolation.
4. Cut the entire skin close to hip flexor and expose the underlying muscle. Remove the

skin and hairs with forceps

5. Cut through the fascia with fine scissors without damaging the underlying Tibialis Anterior (TA). The EDL is found underneath TA.
6. Expose the distal tendons of EDL and TA and cut them with sharp scissors.
7. Hold the distal part of TA and EDL muscles by their tendons and slowly pull the muscles up without stretching towards the proximal.
8. Gently pull the EDL and TA tendons in opposite directions avoiding damage in EDL
9. Transfer EDL to 2 ml of previously prewarmed collagenase solution and place it in incubator set at 37°C and 5% CO₂.
10. For two EDL isolations (one mouse) prepare five plastic Petri dishes (60*15mm) as follows:
11. Prepare six Petri dishes for the isolation (1 for muscle dissociation, 5 for serial washes).
All dishes must be coated with horse serum to prevent myofibers from attaching to plastic.
12. Let it dry for 30 minutes and prewarm DMEM at 37°C
13. Check the muscle and gently shake the muscles in every 30 minutes. Stop the digestion when enough number of single myofiber separate from the EDL. Carefully transfer EDL and myofibers to a prewarmed Petri dish with 4 ml of DMEM (dissociation dish).
14. Transfer single myofiber to DMEM to wash debris and keep it in incubator set at 37°C and 5% CO₂.

IV. In Situ Functional Analysis:

In situ force measurements were performed on both the experimental leg and the contralateral leg following 56 days recovery. CSA and specific tension (SP_O) of the muscle were calculated using the peak tension, weight and length of the lateral gastrocnemius.

Protocol

1. Weigh and anesthetize the animal, and shave both experimental and contralateral hindlimbs.
2. Create a 2 cm skin incision parallel and 2 cm below to the femur to expose the biceps femoris
3. Locate the origin of the biceps femoris and separate the connective tissue with forceps until they go through the biceps femoris.
4. Separate the tissue using hemostats until you can locate the sciatic nerve.
5. Carefully cut the biceps femoris along the femur towards the hip.
6. Isolate the sciatic nerve from surrounding musculature and cut the nerve as close to the hip as possible.
7. Very carefully remove any remaining tissue from the sciatic nerve and tuck it back into place.
8. Make an incision along the midline of posterior portion of the lower limb from the calcaneus to the popliteal region.

9. Separate the skin from the biceps femoris, and cut the biceps femoris similarly to the skin to expose the LGAS.
10. Isolate the gastrocnemius from the biceps femoris.
11. Carefully denervate the MGAS. This will ensure force will be measured only in the LGAS.
12. Cut the calcaneus so that the distal portion of the gastrocnemius and Achilles tendon are still attached.
13. Separate the soleus and plantaris from the GAS by cutting the distal insertions.
14. Using the calcaneus to hold it in place, tie the Achilles tendon to the muscle lever arm of the dual-mode servometer.
15. To stimulate the LGAS, place electrodes connected to a muscle stimulator (Model 2100) on the sciatic nerve.
16. Keep the muscle warm with a radiant heat lamp, and occasionally moisten the muscle and nerve with mineral oil.
17. Using a micrometer, find the muscle's optimal length.
18. Stimulate the LGAS at 150Hz to determine peak tetanic tension. Allow two minutes of rest between contractions.
19. After functional analysis is completed, remove the gastrocnemius and other tissues of interest.
20. Carefully separate the MGAS and LGAS.

21. Weigh muscles and measure the length of the LGAS.

22. Freeze muscles in liquid nitrogen cooled isopentane and store in -80°C freezer.

V. Hematoxylin & Eosin Staining:

Hematoxylin & Eosin staining is one of the most widely used stains in histology to examine skeletal muscle morphology. Hematoxylin stains nucleic acids a dark blue-purplish color. Eosin stains cytoplasm and skeletal myofiber a pink color.

Protocol

1. Immerse slides in Harris Hematoxylin using Coplin jars for five minutes.
2. Immerse slides in tap water until water runs clear.
3. Immerse slides in Eosin for two minutes.
4. Immerse slides in tap water until water runs clear.
5. Immerse slides in 70% ethanol for several seconds. Ethanol will dehydrate the section and remove excess eosin.
6. Immerse slides in 100% ethanol for several seconds.
5. Under the fume hood, immerse slides in Xylene for several seconds. Xylene will make the tissue hydrophobic so a coverslip can be applied with a resin in solvent (PermOUNT).
6. Remove the slides from Xylene and allow slides to dry in the hood.
7. Apply a coverslip using PermOUNT.

Note: Hematoxylin and Eosin can be reused. Do not pour them out; keep them into a

labeled 'used' bottle.

VI. Masson's Trichrome Staining:

Masson's trichrome is a three-color staining to distinguish cells from surrounding connective tissue. This staining produces darkish red keratin and myofibers, blue collagen, light red or pink cytoplasm, and black cell nuclei. It is produced by immersion into Bouin's solution, Weigert's iron hematoxylin, Beibrich scarlett acid fuchsin, phosphotungstic/phosphomolybdic acid, aniline blue and acetic acid.

Protocol

1. Immerse slides in 10% Formalin for 1 hour to fix sections.
2. Re-fix sections in Bouin's solution overnight.
3. Pour out solution and gently rinse slides with tap water to remove yellow color from sections. Then briefly rinse with dH₂O
4. Incubate sections in working Weigert's iron hematoxylin for 5 min.
5. Pour out solution and immerse the slides in water under running tap water to wash out excess of Hematoxylin and to intensify the black color of nuclei. Then rinse with dH₂O for 1 minute
6. Incubate sections in Beibrich Scarlett-Acid Fuchsin for 5 min.
7. Pour out solution and rinse slides in dH₂O for 3x 1 minute
8. Incubate sections in working Phosphotungstic/Phosphomolybdic acid for 30 seconds.

9. Pour out solution and directly immerse sections in Aniline blue for 3 minutes.
10. Pour out solution. Then briefly rinse with dH₂O for 3x 1 minutes.
11. Incubate sections in 1% acetic acid for 2 minutes. Then briefly rinse with dH₂O for 2x 1 minutes.
12. . Dehydrate sections sequentially exposing to a series of solutions for 3 minutes: 70% ethanol, 90% ethanol, 100% ethanol, and xylenes.
13. Dry slides, then mount slides by drops of mounting medium onto slides and covering with coverslips.

VII. Immunohistochemistry

Primary (1°) Antibodies:

- Neurofilament 200: identifies the wide neurofilament in both central and peripheral nerves.
- Sigma, N4142. Stored at -20°C
- PECAM-1 : identifies the endothelial cells and platelets
- BD Pharmingen. Stored at 4°C

Secondary (2°) Antibodies:

- Alexa Fluor® 488 Goat Anti-Rabbit IgG (H+L) Antibody
- Lifetechnologies A-11008. Stored at 4°C

Excitation Wavelengths:

Fluorescein: 488 nm; broad spectrum; easily photobleached

- Donkey Anti-Mouse IgG H&L (TRITC) preadsorbed
- Abcam ab7058. Stored at -20°C
- Absorption Wavelength: 550 nm Emission Wavelength: 570 nm

- Dapi: A fluorescent stain which binds to A-T regions in DNA

Blocking Agents:

- Bovine Serum Albumin (BSA): is able to stabilize enzymatic reactions and enzyme; also prevents adhesion of enzymes from equipment surfaces
 - Fischer Scientific, BP1605-100 Stored at 4°C
- Normal Serum (Goat and Donkey): used to inhibit non-specific binding of antibodies during immunofluorescent staining procedures

Protocol

1. Immerse slides in cold Acetone for 5 minutes.
2. Immediately, rinse slides with PBS 3 times for 5 minutes.
3. Immerse slides in 5% normal serum and 1% BSA in PBS for 1 hour at room temperature.
4. Draw circles around specimen using a barrier pen, in order to keep solutions on the slide.
5. Rinse slides with PBS 3 times for 5 minutes.
6. Incubate tissue slides in PECAM-1 (1:20) or Neurofilament 200 primary antibody (1:200) overnight at 4 °C
7. Rinse slides with PBS 3 times for 5 minutes.
8. Incubate sections for 30 minutes in Alexa 488 secondary antibody (1:200) for 1 hour at room temperature..
9. Rinse with PBS 3 times for 5 minutes.
10. Incubate sections in Dapi (1:1000) for 15 minutes at room temperature
11. Rinse with PBS 3 times for 5 minutes.

APPENDIX B: RAW DATA

1. Entire Region

Cross sectional area

		Entire area (μm^2)	Number of Fiber	Entire area (μm^2)	Number of Fiber	Entire area (μm^2)	Number of Fiber	Entire area (μm^2)	Number of Fiber	Entire area (μm^2)	Number of Fiber
Def	DEF 3	170551	40	177468	40	191363	40	160940	36	209808	47
	DEF 3	211896	47	221613	54	216651	59	223959	50	202345	45
	DEF 3	194501	44	171685	30	138697	28	189161	33	203772	38
	DEF 5	216974	45	197988	36	214307	37	209873	37	195088	34
	DEF 5	186397	42	209393	48	208575	45	213838	46	217335	44
	DEF 5	236306	52	216637	45	215443	38	199135	46	181266	32
	DEF 6	184311	44	199738	42	196443	39	211961	49	228574	49
	DEF 6	184437	47	187771	36	184711	44	207729	42	183227	40
	DEF 6	218516	48	221082	43	226446	43	225352	41	203307	32
	DEF 7	221912	53	218179	49	218817	54	223790	53	208518	47
	DEF 7	222501	53	216001	54	231931	56	213472	58	203776	62
	DEF 7	227268	57	208516	48	214480	50	208011	51	209380	45
INJ	INJ 3	175833	42	195885	51	186261	46	217339	53	199404	43
	INJ 3	184885	41	199934	44	149680	38	157533	35	194980	47
	INJ 3	208263	42	206024	42	178799	42	180194	35	191509	42
	INJ 4	203685	33	194215	33	203367	36	203655	42	197466	39
	INJ 4	167903	39	179675	39	205009	42	185890	44	194781	37
	INJ 4	201824	45	203732	42	215868	40	200793	34	194911	38
	INJ 5	195912	40	193936	39	182252	43	168095	39	199666	42
	INJ 5	192974	38	187900	31	194524	38	181285	33	207041	39
	INJ 5	221456	42	197812	29	164509	31	175515	35	195537	40
	INJ 8	206691	46	181201	43	190757	45	128763	25	160653	51
	INJ 8	177053	38	212284	47	166844	41	194835	46	213626	51
	INJ 8	195966	38	185522	42	184926	40	196410	41	239924	45
EXE	EXE 1	219708	53	201354	43	182713	38	184310	36	213493	34
	EXE 1	181534	33	207336	46	222685	47	188923	43	204908	47
	EXE 1	223633	44	225883	50	212287	45	192939	48	209264	47
	EXE 3	216205	47	209445	41	189859	38	189119	36	196077	40
	EXE 3	193106	44	199036	41	201117	43	193356	39	171718	30
	EXE 3	171389	30	184108	39	203927	42	204568	40	220844	40
	EXE 4	171389	34	184108	31	203927	34	204568	31	220844	30
	EXE 4	172718	36	205655	37	185943	32	205029	34	194621	34
	EXE 4	220628	44	219944	38	178216	28	200267	40	204903	42
	EXE 6	192650	30	202431	39	222598	36	190862	39	198701	37
	EXE 6	219248	46	206828	43	185060	40	210472	54	177834	41
	EXE 6	200566	33	217613	40	225096	49	202665	49	196400	49
INJ+EXE	INJ+EXE 1	202103	45	175779	32	193938	37	196115	38	222129	44
	INJ+EXE 1	218933	43	190336	44	225673	50	211927	48	205795	49
	INJ+EXE 1	184488	40	184999	41	177990	33	184064	37	206586	37
	INJ+EXE 2	181890	34	207880	38	181289	35	213671	41	176892	24
	INJ+EXE 2	180783	30	156423	26	209473	49	202064	37	202726	38
	INJ+EXE 2	172876	46	185676	36	178640	27	149217	28	148651	36
	INJ+EXE 3	192848	45	212445	41	198710	38	185611	35	221271	39
	INJ+EXE 3	163095	38	136848	30	199068	42	149538	34	157016	39
	INJ+EXE 3	193029	47	165940	42	178785	43	215165	47	205994	41
	INJ+EXE 5	194515	46	208857	49	211319	52	190894	48	209755	46
	INJ+EXE 5	198332	36	209778	54	120753	33	197134	56	175665	47
	INJ+EXE 5	200590	48	205839	47	186454	46	195419	49	193120	42

Nerve CSA (µm2) and number

INJ 3	INJ 4	INJ 5	INJ+EXE 1	INJ+EXE 2	INJ+EXE 3	DEF 3	DEF 5	DEF 6	EXE 1	EXE 3	EXE 5
59570	1233	2673	461	1281	1079	17361	1575	1282	755	896	4926
4150	1197	1360	56563	287	5959	38207	1622	513	1825	765	2760
1266	430	244	6130	290	17419	2515	125	222	403	711	981
994	2099	214	3719	230	1712	370	345	4056	427	342	20348
1216	863	619	14974	2177	2219	392	243	1134	4095	1442	3656
16522	58556	1399	310	636	5737	638	1808	1494	5539	827	956
1113	5033	270	354	551	846	695	64439	819	16448	619	3659
576	329	387	250	132	2579	701	5386	738	2391	1744	658
47325	312	2144	692	627	1605	3518	12450	14487	763	995	1752
1217	236	5501	352	679	587	320	226	5910	1592	96715	423
2433	105	72158	137	2718	2503	462	545	838	1000	1410	255
873	516	18467	473	27414	421	1127	1744	424	20208	1239	562
788	864	1604	2858	2034	564	1161	1245	278	35033	18618	867
14322	4832	770	913	218	7029	343	792	1632	12427	1390	1465
772	351	11630	164	5552	1865	364	701	1269	22146	4223	1947
1393	24760	559	1376	13983	117138	615	688	2471	8743	1486	234
577	1153	2900	503	2302	8921	53749	519	7255	6463	525	490
104	296	2628	216	615	1539	3978	662	1500	888	494	844
764	621	2484	6320	232	408	14282	289	724	19896	20057	445
254	486	232	61511	1491	556	680	1998	93941	6366	9310	2067
567	1199	343	1204	1889	407	258	260	8321	550	1459	458
289	20980	1024	300	449	244	368	529	11005	8429	1235	357
812	698	518	803	485	5727	853	1642	10597	18375	2599	333
386	37764	1258	516	19259	218	2509	17731	67536	9963	3968	862
2044	201	369	642	6385	395	305	56513	4914	5464	577	790
2668	11767	4535	17048	68254	709	269	1596	3874	500	447	385
2203	356	60061	664	23006	395	727	292	489	11827	962	4291
314	1827	34871	792	10630	21033	697	2293	367	7207	289	1010
417	2158	542	341	313	4189	1122	627	1048	484	371	460
15541	693	565	353	669	372	255	20190	715	1278	780	2298
662	81	3132	637	653	620	510	2989	481	40741	968	13503
907	1241	314	1154	152	1034	12516	680	874	1164	639	3755
495	3930	669	7841	528	463	8225	443	573	1223	466	2386
1743	316	566	1220	1221	272	57506	320	14974	1290	1270	351
67380	25775	830	3128	2276	58776	4166	423	886	860	73521	435
	1326	422	1070	46363	3977	1583	943	446	568	12581	496
	86401	3284	54129	6619	274		2923	78259	594	4889	1313
	3099	5363	7069	2708	466		549	3426	999	4406	198
		288	571	691	909		17409	1142		553	362
		13658	293	1717	342		51657	715		2298	9474
		14562	326	627	5382		19841	731		1813	55320
		3902		791	322		609	793		824	21189
		458		1480	365		406	595		292	567
		730		226	302		2432	926		297	575
		1508		274	660			1159		351	631
		289		182	191			1125		430	1549
		3834			394			373		195	432
		935			1451					16937	1645
		509			589					4166	513
		331			1095					19836	1137
		756			312					8232	381
		95655			623					248	4079
					254					186	205
										272	352
										50365	1274
											1119
											415
											898
											956
											317
											1128
											242
											332
											5986
											4311
											1154
											21705
											45371

Number of blood vessel

		Regenerating area	Entire Area
Def	DEF 3	7	43
	DEF 3	17	32
	DEF 3	14	36
	DEF 5	11	13
	DEF 5	7	7
	DEF 5	12	17
	DEF 6	14	16
	DEF 6	15	19
	DEF 6	22	21
	DEF 7	4	12
	DEF 7	11	33
	DEF 7	7	12
INJ	INJ 3	11	20
	INJ 3	13	32
	INJ 3	5	13
	INJ 4	4	24
	INJ 4	19	32
	INJ 4	15	42
	INJ 5	8	26
	INJ 5	7	26
	INJ 5	11	25
	INJ 8	7	20
	INJ 8	8	31
	INJ 8	9	25
EXE	EXE 1	7	35
	EXE 1	15	28
	EXE 1	13	60
	EXE 3	5	14
	EXE 3	11	28
	EXE 3	14	30
	EXE 4	4	27
	EXE 4	6	38
	EXE 4	17	30
	EXE 6	21	45
	EXE 6	14	34
	EXE 6	17	42
INJ+ EXE	INJ+ EXE 1	8	14
	INJ+ EXE 1	14	20
	INJ+ EXE 1	11	31
	INJ+ EXE 2	5	21
	INJ+ EXE 2	9	19
	INJ+ EXE 2	12	28
	INJ+ EXE 3	7	25
	INJ+ EXE 3	10	18
	INJ+ EXE 3	9	24
	INJ+ EXE 5	11	33
	INJ+ EXE 5	10	30
	INJ+ EXE 5	15	32

2. Middel Region

% Fibrosis			
ECM	FIB	EXE	FIB+EXE
69	57	48	52
69	69	45	65
74	42	43	74
65	50	–	64

Small Muscle Area (mm2)

ECM	FIB	EXE	FIB+EXE
0.490	0.974	1.503	1.332
0.300	0.273	1.076	0.610
0.689	0.870	1.595	0.421
0.485	0.566	–	0.750

Nerve			
ECM	FIB	EXE	FIB+EXE
15	18	15	13
15	8	14	18
11	4	12	3

Number of Blood Vessel

Entire Area			
ECM	FIB	EXE	FIB+EXE
49	45	43	34
14	51	39	28
34	33	44	28
44	39		40
Regenerating Area			
ECM	FIB	EXE	FIB+EXE
32	32	28	20
7	32	28	19
19	26	38	18
33	31		30

References

- Äärimaa, V., et al. (2004). "Restoration of myofiber continuity after transection injury in the rat soleus." Neuromuscular Disorders **14**(7): 421-428.
- Aagaard, P., et al. (2002). "Increased rate of force development and neural drive of human skeletal muscle following resistance training." Journal of Applied Physiology **93**(4): 1318-1326.
- Acheson, A., et al. (1995). "A BDNF autocrine loop in adult sensory neurons prevents cell death."
- Allen, R. E. and L. K. Boxhorn (1989). "Regulation of skeletal muscle satellite cell proliferation and differentiation by transforming growth factor-beta, insulin-like growth factor I, and fibroblast growth factor." Journal of cellular physiology **138**(2): 311-315.
- Allen, R. E., et al. (1995). "Hepatocyte growth factor activates quiescent skeletal muscle satellite cells in vitro." Journal of cellular physiology **165**(2): 307-312.
- Amaral, S. L., et al. (2001). "Angiotensin II and VEGF are involved in angiogenesis induced by short-term exercise training." American Journal of Physiology-Heart and Circulatory Physiology **281**(3): H1163-H1169.
- Arnold, L., et al. (2007). "Inflammatory monocytes recruited after skeletal muscle injury switch into antiinflammatory macrophages to support myogenesis." The Journal of experimental medicine **204**(5): 1057-1069.
- Badylak, S., et al. (2003). Extracellular matrix for myocardial repair. The heart surgery forum, Carden Jennings.
- Badylak, S. F., et al. (2008). "Macrophage phenotype as a determinant of biologic scaffold remodeling." Tissue Engineering Part A **14**(11): 1835-1842.
- Beattie, A. J., et al. (2008). "Chemoattraction of progenitor cells by remodeling extracellular matrix scaffolds." Tissue Engineering Part A **15**(5): 1119-1125.
- Belperio, J. A., et al. (2002). "Critical role for CXCR2 and CXCR2 ligands during the pathogenesis of ventilator-induced lung injury." Journal of Clinical Investigation **110**(11): 1703-1716.

Biressi, S. and T. A. Rando (2010). Heterogeneity in the muscle satellite cell population. Seminars in cell & developmental biology, Elsevier.

Bischoff, R. (1997). "Chemotaxis of skeletal muscle satellite cells." Developmental dynamics **208**(4): 505-515.

Boldrin, L. and J. E. Morgan (2013). "Grafting of a Single Donor Myofibre Promotes Hypertrophy in Dystrophic Mouse Muscle." PloS one **8**(1): e54599.

Borisov, A. B., et al. (2005). "Abortive myogenesis in denervated skeletal muscle: differentiative properties of satellite cells, their migration, and block of terminal differentiation." Anatomy and embryology **209**(4): 269-279.

Borschel, G. H., et al. (2004). "Contractile skeletal muscle tissue-engineered on an acellular scaffold." Plastic and reconstructive surgery **113**(2): 595-602.

Borselli, C., et al. (2010). "Functional muscle regeneration with combined delivery of angiogenesis and myogenesis factors." Proceedings of the National Academy of Sciences **107**(8): 3287-3292.

Brzóśka, E., et al. (2006). "Integrin $\alpha 3$ subunit participates in myoblast adhesion and fusion in vitro." Differentiation **74**(2-3): 105-118.

Cannon, J. G. and B. A. S. Pierre (1998). "Cytokines in exertion-induced skeletal muscle injury." Molecular and cellular biochemistry **179**(1-2): 159-168.

Carlson, B. M. and J. A. Faulkner (1982). "The regeneration of skeletal muscle fibers following injury: a review." Medicine and science in sports and exercise **15**(3): 187-198.

Carmeliet, P. and R. K. Jain (2000). "Angiogenesis in cancer and other diseases." Nature **407**(6801): 249-257.

Charge, S. B. and M. A. Rudnicki (2004). "Cellular and molecular regulation of muscle regeneration." Physiological reviews **84**(1): 209-238.

Chazaud, B., et al. (2009). "Dual and beneficial roles of macrophages during skeletal muscle regeneration." Exercise and sport sciences reviews **37**(1): 18-22.

Chen, X. K. and T. J. Walters (2013). "Muscle-derived decellularised extracellular matrix

improves functional recovery in a rat latissimus dorsi muscle defect model." Journal of Plastic, Reconstructive & Aesthetic Surgery **66**(12): 1750-1758.

Clark, K. A., et al. (2002). "Striated muscle cytoarchitecture: an intricate web of form and function." Annual review of cell and developmental biology **18**(1): 637-706.

Collins, C. A., et al. (2005). "Stem cell function, self-renewal, and behavioral heterogeneity of cells from the adult muscle satellite cell niche." Cell **122**(2): 289-301.

Collins, C. A., et al. (2007). "A population of myogenic stem cells that survives skeletal muscle aging." Stem Cells **25**(4): 885-894.

Conconi, M. T., et al. (2005). "Homologous muscle acellular matrix seeded with autologous myoblasts as a tissue-engineering approach to abdominal wall-defect repair." Biomaterials **26**(15): 2567-2574.

Cooper, R., et al. (1999). "In vivo satellite cell activation via Myf5 and MyoD in regenerating mouse skeletal muscle." Journal of cell science **112**(17): 2895-2901.

Coppi, P. D., et al. (2006). "Myoblast-acellular skeletal muscle matrix constructs guarantee a long-term repair of experimental full-thickness abdominal wall defects." Tissue engineering **12**(7): 1929-1936.

Cornelison, D., et al. (2000). "MyoD^{-/-} satellite cells in single-fiber culture are differentiation defective and MRF4 deficient." Developmental biology **224**(2): 122-137.

Cornelison, D. and B. J. Wold (1997). "Single-cell analysis of regulatory gene expression in quiescent and activated mouse skeletal muscle satellite cells." Developmental biology **191**(2): 270-283.

Corona, B. T., et al. (2013). "The promotion of a functional fibrosis in skeletal muscle with volumetric muscle loss injury following the transplantation of muscle-ECM." Biomaterials **34**(13): 3324-3335.

Crow, B. D., et al. (2007). "Evaluation of a novel biomaterial for intrasubstance muscle laceration repair." Journal of orthopaedic research **25**(3): 396-403.

Darr, K. C. and E. Schultz (1987). "Exercise-induced satellite cell activation in growing and mature skeletal muscle." Journal of Applied Physiology **63**(5): 1816-1821.

Duncan, N. D., et al. (1998). "Adaptations in rat skeletal muscle following long-term resistance exercise training." European journal of applied physiology and occupational physiology **77**(4): 372-378.

Engler, A. J., et al. (2006). "Matrix elasticity directs stem cell lineage specification." Cell **126**(4): 677-689.

Folland, J. P. and A. G. Williams (2007). "Morphological and neurological contributions to increased strength." Sports Medicine **37**(2): 145-168.

Friedrich, J. B., et al. (2011). "Reconstruction of soft-tissue injury associated with lower extremity fracture." Journal of the American Academy of Orthopaedic Surgeons **19**(2): 81-90.

Fry, A. C. (2004). "The role of resistance exercise intensity on muscle fibre adaptations." Sports Medicine **34**(10): 663-679.

Gibson, M. C. and E. Schultz (1982). "The distribution of satellite cells and their relationship to specific fiber types in soleus and extensor digitorum longus muscles." The Anatomical Record **202**(3): 329-337.

Gilbert, T. W., et al. (2009). "Quantification of DNA in biologic scaffold materials." Journal of Surgical Research **152**(1): 135-139.

Green, H., et al. (1999). "Regulation of fiber size, oxidative potential, and capillarization in human muscle by resistance exercise." American Journal of Physiology-Regulatory, Integrative and Comparative Physiology **276**(2): R591-R596.

Grefte, S., et al. (2007). "Skeletal muscle development and regeneration." Stem cells and development **16**(5): 857-868.

Grogan, B. F., et al. (2011). "Volumetric muscle loss." Journal of the American Academy of Orthopaedic Surgeons **19**(suppl 1): S35-S37.

Grounds, M. D., et al. (1992). "Identification of skeletal muscle precursor cells in vivo by use of MyoD1 and myogenin probes." Cell and tissue research **267**(1): 99-104.

Hall, J. K., et al. (2010). "Prevention of muscle aging by myofiber-associated satellite cell transplantation." Science translational medicine **2**(57): 57ra83-57ra83.

Hasty, P., et al. (1993). "Muscle deficiency and neonatal death in mice with a targeted

mutation in the myogenin gene."

Hawke, T. J. and D. J. Garry (2001). "Myogenic satellite cells: physiology to molecular biology." Journal of Applied Physiology **91**(2): 534-551.

Herdy, A. H., et al. (2008). "Pre-and postoperative cardiopulmonary rehabilitation in hospitalized patients undergoing coronary artery bypass surgery: a randomized controlled trial." American Journal of Physical Medicine & Rehabilitation **87**(9): 714-719.

Hinds, S., et al. (2011). "The role of extracellular matrix composition in structure and function of bioengineered skeletal muscle." Biomaterials **32**(14): 3575-3583.

Ho, K. W., et al. (1980). "Skeletal muscle fiber splitting with weight-lifting exercise in rats." American Journal of Anatomy **157**(4): 433-440.

Hornberger Jr, T. A. and R. P. Farrar (2004). "Physiological hypertrophy of the FHL muscle following 8 weeks of progressive resistance exercise in the rat." Canadian journal of applied physiology **29**(1): 16-31.

Huang, E. J. and L. F. Reichardt (2001). "Neurotrophins: roles in neuronal development and function." Annual review of neuroscience **24**: 677.

Huard, J., et al. (2002). "Muscle injuries and repair: current trends in research." The Journal of Bone & Joint Surgery **84**(5): 822-832.

Hurme, T., et al. (1991). "Healing of skeletal muscle injury: an ultrastructural and immunohistochemical study." Medicine and science in sports and exercise **23**(7): 801-810.

Järvinen, T. A., et al. (2005). "Muscle injuries biology and treatment." The American journal of sports medicine **33**(5): 745-764.

Jacobson, C., et al. (2004). "Neuregulin induces the expression of transcription factors and myosin heavy chains typical of muscle spindles in cultured human muscle." Proceedings of the National Academy of Sciences of the United States of America **101**(33): 12218-12223.

Jostes, B., et al. (1990). "The murine paired box gene, Pax7, is expressed specifically during the development of the nervous and muscular system." Mechanisms of development **33**(1): 27-37.

Juhas, M. and N. Bursac (2013). "Engineering skeletal muscle repair." Current opinion in

biotechnology **24**(5): 880-886.

Kääriäinen, M., et al. (2000). "Relation between myofibers and connective tissue during muscle injury repair." Scandinavian journal of medicine & science in sports **10**(6): 332-337.

KIEFER, F. N., et al. (2002). "Hypoxia enhances vascular cell proliferation and angiogenesis in vitro via rapamycin (mTOR)-dependent signaling." The FASEB Journal **16**(8): 771-780.

Kilmer, D. D., et al. (1994). "The effect of a high resistance exercise program in slowly progressive neuromuscular disease." Archives of physical medicine and rehabilitation **75**(5): 560-563.

Kim, M. S., et al. (2001). "Histone deacetylases induce angiogenesis by negative regulation of tumor suppressor genes." Nature medicine **7**(4): 437-443.

Kjær, M. (2004). "Role of extracellular matrix in adaptation of tendon and skeletal muscle to mechanical loading." Physiological reviews **84**(2): 649-698.

Kochupura, P. V., et al. (2005). "Tissue-engineered myocardial patch derived from extracellular matrix provides regional mechanical function." Circulation **112**(9 suppl): I-144-I-149.

Kopp, D. M., et al. (1997). "Glial growth factor rescues Schwann cells of mechanoreceptors from denervation-induced apoptosis." The Journal of neuroscience **17**(17): 6697-6706.

Kragh Jr, J. F., et al. (2005). "Epimysium and perimysium in suturing in skeletal muscle lacerations." Journal of trauma and acute care surgery **59**(1): 209-212.

Larkin, L. M., et al. (2003). "Effects of age and nerve-repair grafts on reinnervation and fiber type distribution of rat medial gastrocnemius muscles." Mechanisms of ageing and development **124**(5): 653-661.

Laufs, U., et al. (2004). "Physical training increases endothelial progenitor cells, inhibits neointima formation, and enhances angiogenesis." Circulation **109**(2): 220-226.

Laughlin, M. and B. Roseguini (2008). "Mechanisms for exercise training-induced increases in skeletal muscle blood flow capacity: differences with interval sprint training versus aerobic endurance training." Journal of physiology and pharmacology: an official journal of the Polish Physiological Society **59**(Suppl 7): 71.

Lavasani, M., et al. (2006). "Nerve growth factor improves the muscle regeneration capacity of muscle stem cells in dystrophic muscle." Human gene therapy **17**(2): 180-192.

Lee, S., et al. (2004). "Viral expression of insulin-like growth factor-I enhances muscle hypertrophy in resistance-trained rats." Journal of Applied Physiology **96**(3): 1097-1104.

Li, X., et al. (2008). "Extracellular matrix proteoglycan decorin-mediated myogenic satellite cell responsiveness to transforming growth factor- β 1 during cell proliferation and differentiation: Decorin and transforming growth factor- β 1 in satellite cells." Domestic animal endocrinology **35**(3): 263-273.

Li, X., et al. (2007). "Effects of hypoxia on proliferation and differentiation of myoblasts." Medical hypotheses **69**(3): 629-636.

Lindström, M., et al. (2010). "Satellite cell heterogeneity with respect to expression of MyoD, myogenin, Dlk1 and c-Met in human skeletal muscle: application to a cohort of power lifters and sedentary men." Histochemistry and cell biology **134**(4): 371-385.

Lolmede, K., et al. (2009). "Inflammatory and alternatively activated human macrophages attract vessel-associated stem cells, relying on separate HMGB1-and MMP-9-dependent pathways." Journal of leukocyte biology **85**(5): 779-787.

Lucia, A., et al. (2009). "Mobilisation of mesenchymal cells in cardiac patients: is intense exercise necessary?" British journal of sports medicine **43**(3): 221-223.

MacDougall, J. D., et al. (1995). "The time course for elevated muscle protein synthesis following heavy resistance exercise." Canadian journal of applied physiology **20**(4): 480-486.

Mackey, A., et al. (2007). "Enhanced satellite cell proliferation with resistance training in elderly men and women." Scandinavian journal of medicine & science in sports **17**(1): 34-42.

Marzaro, M., et al. (2002). "Autologous satellite cell seeding improves in vivo biocompatibility of homologous muscle acellular matrix implants." International journal of molecular medicine **10**(2): 177-182.

Mase Jr, V. J., et al. (2010). "Clinical application of an acellular biologic scaffold for surgical repair of a large, traumatic quadriceps femoris muscle defect." Orthopedics **33**(7): 511-511.

Mauney, J., et al. (2010). "Matrix remodeling as stem cell recruitment event: a novel in vitro model for homing of human bone marrow stromal cells to the site of injury shows crucial role of extracellular collagen matrix." Matrix Biology **29**(8): 657-663.

Mauro, A. (1961). "Satellite cell of skeletal muscle fibers." The Journal of biophysical and biochemical cytology **9**(2): 493-495.

McCall, G., et al. (1996). "Muscle fiber hypertrophy, hyperplasia, and capillary density in college men after resistance training." Journal of Applied Physiology **81**(5): 2004-2012.

McFarland, D. C., et al. (1988). "The turkey myogenic satellite cell: optimization of in vitro proliferation and differentiation." Tissue and Cell **20**(6): 899-908.

Megeney, L. A., et al. (1996). "MyoD is required for myogenic stem cell function in adult skeletal muscle." Genes & development **10**(10): 1173-1183.

Meintjes, J., et al. (2011). "Synthetic, biological and composite scaffolds for abdominal wall reconstruction." Expert review of medical devices **8**(2): 275-288.

Merritt, E. K., et al. (2010). "Repair of traumatic skeletal muscle injury with bone-marrow-derived mesenchymal stem cells seeded on extracellular matrix." Tissue Engineering Part A **16**(9): 2871-2881.

Merritt, E. K., et al. (2010). "Functional assessment of skeletal muscle regeneration utilizing homologous extracellular matrix as scaffolding." Tissue Engineering Part A **16**(4): 1395-1405.

Messina, S., et al. (2007). "VEGF overexpression via adeno-associated virus gene transfer promotes skeletal muscle regeneration and enhances muscle function in mdx mice." The FASEB Journal **21**(13): 3737-3746.

Montarras, D., et al. (2005). "Direct isolation of satellite cells for skeletal muscle regeneration." Science **309**(5743): 2064-2067.

Mouly, V., et al. (2005). "The mitotic clock in skeletal muscle regeneration, disease and cell mediated gene therapy." Acta physiologica scandinavica **184**(1): 3-15.

Musarò, A. (2014). "The basis of muscle regeneration." Advances in Biology **2014**.

Nabeshima, Y., et al. (1993). "Myogenin gene disruption results in perinatal lethality because of severe muscle defect."

Nandan, D., et al. (1990). "Ethyl-3, 4-dihydroxybenzoate inhibits myoblast differentiation: evidence for an essential role of collagen." The Journal of cell biology **110**(5): 1673-1679.

Norris, B. L. and J. F. Kellam (1997). "Soft-tissue injuries associated with high-energy extremity trauma: principles of management." Journal of the American Academy of Orthopaedic Surgeons **5**(1): 37-46.

Park, J. S., et al. (2011). "The effect of matrix stiffness on the differentiation of mesenchymal stem cells in response to TGF- β ." Biomaterials **32**(16): 3921-3930.

Petrella, J. K., et al. (2008). "Potent myofiber hypertrophy during resistance training in humans is associated with satellite cell-mediated myonuclear addition: a cluster analysis." Journal of Applied Physiology **104**(6): 1736-1742.

Quintero, A. J., et al. (2009). "Stem cells for the treatment of skeletal muscle injury." Clinics in sports medicine **28**(1): 1-11.

Rigamonti, E., et al. (2014). "Macrophage plasticity in skeletal muscle repair." BioMed research international **2014**.

Rossi, C. A., et al. (2010). "Clonal characterization of rat muscle satellite cells: proliferation, metabolism and differentiation define an intrinsic heterogeneity." PLoS One **5**(1): e8523.

Ruberti, F., et al. (2000). "Phenotypic knockout of nerve growth factor in adult transgenic mice reveals severe deficits in basal forebrain cholinergic neurons, cell death in the spleen, and skeletal muscle dystrophy." The Journal of neuroscience **20**(7): 2589-2601.

Sabourin, L. A., et al. (1999). "Reduced differentiation potential of primary MyoD^{-/-} myogenic cells derived from adult skeletal muscle." The Journal of cell biology **144**(4): 631-643.

Sacco, A., et al. (2008). "Self-renewal and expansion of single transplanted muscle stem cells." Nature **456**(7221): 502-506.

Schmalbruch, H. and U. Hellhammer (1977). "The number of nuclei in adult rat muscles with special reference to satellite cells." The Anatomical Record **189**(2): 169-175.

Schultz, E. (1974). "A quantitative study of the satellite cell population in postnatal mouse lumbrical muscle." The Anatomical Record **180**(4): 589-595.

Schultz, G. S. and A. Wysocki (2009). "Interactions between extracellular matrix and growth factors in wound healing." Wound repair and regeneration **17**(2): 153-162.

Seale, P., et al. (2000). "Pax7 is required for the specification of myogenic satellite cells." Cell **102**(6): 777-786.

Shimizu, S., et al. (2007). "Peripheral nerve regeneration by the in vitro differentiated-human bone marrow stromal cells with Schwann cell property." Biochemical and biophysical research communications **359**(4): 915-920.

Sica, A. and A. Mantovani (2012). "Macrophage plasticity and polarization: in vivo veritas." The Journal of clinical investigation **122**(122 (3)): 787-795.

Siegel, A. L., et al. (2009). "3D timelapse analysis of muscle satellite cell motility." Stem Cells **27**(10): 2527-2538.

Snow, M. H. (1983). "A quantitative ultrastructural analysis of satellite cells in denervated fast and slow muscles of the mouse." The Anatomical Record **207**(4): 593-604.

Son, Y.-J. and W. J. Thompson (1995). "Nerve sprouting in muscle is induced and guided by processes extended by Schwann cells." Neuron **14**(1): 133-141.

Stern, M. M., et al. (2009). "The influence of extracellular matrix derived from skeletal muscle tissue on the proliferation and differentiation of myogenic progenitor cells ex vivo." Biomaterials **30**(12): 2393-2399.

Tamaki, T., et al. (2005). "Functional recovery of damaged skeletal muscle through synchronized vasculogenesis, myogenesis, and neurogenesis by muscle-derived stem cells." Circulation **112**(18): 2857-2866.

Taylor, M. D., et al. (2001). "Postnatal regulation of limb proprioception by muscle-derived neurotrophin-3." Journal of Comparative Neurology **432**(2): 244-258.

Tedesco, F. S., et al. (2010). "Repairing skeletal muscle: regenerative potential of skeletal muscle stem cells." The Journal of clinical investigation **120**(1): 11.

Teixeira, C., et al. (2003). "Neutrophils do not contribute to local tissue damage, but play a key role in skeletal muscle regeneration, in mice injected with Bothrops asper snake venom." Muscle & nerve **28**(4): 449-459.

TENNYSON, V. M., et al. (1973). "ACETYLCHOLINESTERASE ACTIVITY IN THE MYOTUBE AND MUSCLE SATELLITE CELL OF THE FETAL RABBIT AN

ELECTRON MICROSCOPIC-CYTOCHEMICAL AND BIOCHEMICAL STUDY." Journal of Histochemistry & Cytochemistry **21**(7): 634-652.

Terada, S. T., Harumoto Yamada, Tsuneo Seki, Nobuki (2001). "Muscle repair after a transection injury with development of a gap: an experimental study in rats." Scandinavian journal of plastic and reconstructive surgery and hand surgery **35**(3): 233-238.

Thornell, L. E., et al. (2003). "Satellite cells and training in the elderly." Scandinavian journal of medicine & science in sports **13**(1): 48-55.

Tidball, J. G. (2005). "Inflammatory processes in muscle injury and repair." American Journal of Physiology-Regulatory, Integrative and Comparative Physiology **288**(2): R345-R353.

Tidball, J. G. and S. A. Villalta (2010). "Regulatory interactions between muscle and the immune system during muscle regeneration." American Journal of Physiology-Regulatory, Integrative and Comparative Physiology **298**(5): R1173-R1187.

Trachtenberg, J. T. and W. J. Thompson (1996). "Schwann cell apoptosis at developing neuromuscular junctions is regulated by glial growth factor." Nature **379**(6561): 174-177.

Vaittinen, S., et al. (2002). "Transected myofibres may remain permanently divided in two parts." Neuromuscular Disorders **12**(6): 584-587.

Venuti, J. M., et al. (1995). "Myogenin is required for late but not early aspects of myogenesis during mouse development." The Journal of cell biology **128**(4): 563-576.

Yablonka-Reuveni, Z., et al. (1999). "Fibroblast growth factor promotes recruitment of skeletal muscle satellite cells in young and old rats." Journal of Histochemistry & Cytochemistry **47**(1): 23-42.

Yarrow, J. F., et al. (2010). "Training augments resistance exercise induced elevation of circulating brain derived neurotrophic factor (BDNF)." Neuroscience letters **479**(2): 161-165.

Yu, X., et al. (1999). "A laminin and nerve growth factor-laden three-dimensional scaffold for enhanced neurite extension." Tissue engineering **5**(4): 291-304.

Zammit, P. S., et al. (2002). "Kinetics of myoblast proliferation show that resident satellite cells are competent to fully regenerate skeletal muscle fibers." Experimental cell research **281**(1): 39-49.